China Geology 9 (2026) 175−194

China Geology

Journal homepage: http://chinageology.cgs.cn
https://www.sciencedirect.com/journal/china-geology

Geology, carbon emission reduction potential, and development progress of hot dry rock in China

Wen-jing Lin[a, b,*], Ya-ru Wang[a, b], Rui Lu[c], Sheng-sheng Zhang[d], Gui-ling Wang[a, b]

[a] *Institute of Hydrogeology and Environmental Geology*, *Chinese Academy of Geological Sciences*, *Shijiazhuang* 050061, *China*
[b] *Technology Innovation Center for Geothermal & Hot Dry Rock Exploration and Development*, *Ministry of Natural Resources*, *Shijiazhuang* 050061, *China*
[c] *Qinghai Geological Survey Bureau*, *Xining* 810000, *China*
[d] *Institute of the Hydrogeology and Engineering Geology of Qinghai*, *Xining* 810000, *China*

A R T I C L E I N F O

Article history:
Received 8 February 2024
Received in revised form 6 April 2024
Accepted 27 April 2024
Available online 19 July 2025

Keywords:
Hot dry rock
Highly radioactive heat-producing type
Sedimentary basin type
Active volcanic type
Intensely tectonic zone type
Clean energy
Power generation
Exploration progress
Enhanced geothermal system (EGS)
Carbon reduction potential

A B S T R A C T

The available heat content (stored heat energy) of hot dry rock (HDR) at a depth of 1–10 km in the global land crust is estimated to be 5.06 × 10^8 EJ, attracting considerable global attention. This paper presents a comprehensive analysis of the geological framework, HDR resource potential, exploration advancements, and the development of enhanced geothermal systems (EGSs) in China. HDR resources are extensively distributed across China. Within the depth range of 3–10 km, China's estimated potential approximates 2.29 × 10^7 EJ, with a theoretical power generation capacity of approximately 1.67 × 10^{16} kWh. Replacing coal power with HDR can help to achieve a net emission reduction of 1.34 × 10^{16} kg CO_2 (approximately 1.34 × 10^{13} t), representing an emission reduction efficiency of 94.4%. Based on a development cycle of 100 years, the average annual emission reduction reaches 1.34 × 10^{10} t CO_2, equivalent to 117% of China's annual carbon emissions in 2022. Furthermore, in the context of global warming, the development and utilization of HDR, which is feasible in virtually any region worldwide, offers significant potential to support global carbon reduction efforts. China has made substantial progress in HDR exploration in recent years. This paper systematically classifies China's HDR resources into four genetic types —highly radioactive heat-producing, sedimentary basin, active volcanic, and intensely tectonic zones—and offers detailed exploration insights for each category. Each classification exhibits distinct geological and tectonic characteristics that influence heat source mechanisms and resource distribution. Furthermore, this paper documents significant advances in EGS construction, particularly in the Gonghe Basin on the northeastern margin of the Qianghai-Xizang Plateau and the Matouying uplift in the North China Basin, where successful reservoir stimulation, microseismic monitoring, and experimental power generation have been achieved. Despite these developments, challenges persist, including technical adaptability under complex geological conditions and the economic viability of large-scale HDR development. This paper suggests that future initiatives should emphasize resource exploration, technological research, and policy support to foster sustainable HDR resource development in China, thereby contributing to the global energy transition and environmental sustainability.

©2026 China Geology Editorial Office.

1. Introduction

Hot dry rock (HDR) geothermal energy was first conceptualized at Los Alamos National Laboratory in the early 1970s as a means to harness heat from large areas of the earth's crust that lack natural fluids —regions far more extensive than conventional hydrothermal resources (Brown DW, 2009). HDR exhibits widespread distribution and represents the primary trajectory for future geothermal development (Tester JW et al., 2006). The available heat content (stored thermal energy) of HDR at depths of 1–10 km in the global land crust is estimated to be 5.06 × 10^8 EJ (Aghahosseini A and Breyer C, 2020). This substantial resource potential holds strategic significance for global carbon neutrality objectives, and its stable power supply characteristics effectively complement the intermittent nature of renewable energy sources, facilitating deep decarbonization of the energy system. Particularly for coal-dependent economies such as China and India, large-scale HDR

First author: *E-mail address*: linwenjing@mail.cgs.gov.cn (Wen-jing Lin).

* Corresponding author: *E-mail address*: linwenjing@mail.cgs.gov.cn (Wen-jing Lin).

Literary editor: Xi-jie Chen
doi:10.31035/cg2024100
2096-5192/© 2026 China Geology Editorial Office.

Copyright © 2026 Editorial Office of China Geology. Publishing services by Elsevier B.V. on behalf of KeAi Communications Co. Ltd.
This is an open access article under the CC BY-NC-ND License (http://creativecommons.org/licenses/by-nc-nd/4.0/).

development can accelerate coal power substitution and mitigate the carbon lock-in effect. Consequently, amid continuing global warming, the exploitation and utilization of HDR, which is feasible in virtually any region worldwide, will substantially contribute to future global carbon reduction efforts.

Due to current technological constraints, the HDR accessible for human exploitation primarily consists of underground high-temperature rocks at economically viable depths. China's geographical position at the intersection of the Pacific Rim and Mediterranean-Himalayan geothermal zones gives it access to abundant high-temperature hydrothermal resources, especially in the Qinghai-Xizang Plateau region (Zhang XB and Hu QH, 2018). Water-impermeable high-temperature rocks or those containing minimal vapor often form adjacent to these high-temperature hydrothermal systems, presenting opportunities for HDR development (Wang GL and Lin WJ, 2020). Furthermore, China's territory encompasses extensive Meso-Cenozoic and Cenozoic sedimentary basins, notably the rift-type basins in the eastern region, including the North China Basin, Songliao Basin, Jianghan Basin, and North Jiangsu Basin. Their substantial sedimentary layers create favorable conditions for heat retention (Zhang W et al., 2019). These geological characteristics indicate significant potential for HDR resources in China.

Despite China's relatively recent entry into HDR exploration and development, it has achieved substantial progress. Wan ZJ et al. (2005) conducted the initial study of China's HDR resource potential zones, identifying favorable HDR development zones, including southern Xizang, Tengchong in western Yunnan Province, northern Hainan Province, Changbaishan in Jilin Province, and Wudalianchi in Heilongjiang Province, as prospective HDR geothermal resource zones. Lin WJ et al. (2012) evaluated the HDR resource potential within China's land area to a depth of 10 km using the volumetric method, revealing extensive development potential. Wang GL et al. (2016) established four HDR genesis types: highly radioactive heat-producing, sedimentary basin, active volcanic, and strongly tectonically active zones, based on global HDR discoveries and China's geological context. Lin WJ et al. (2023) examined the heat source mechanisms of various HDR types in China, identifying primary heat-controlling geological factors across different tectonic zones. These studies have established a foundation for HDR exploration, site selection, and enhanced geothermal system (EGS) development in China through the analysis of geological backgrounds, resource potential, and genesis modes.

HDR surveys have been implemented across various regions. Li WB (2016) conducted HDR surveys of the Cangxian uplift in the North China Basin, successfully performed hydraulic fracturing of deep carbonate geothermal reservoirs, established China's first EGS, and achieved geothermal power generation with cascade utilization (Qin XX et al., 2019). Jiang HY et al. (2019) investigated HDR in the Shandong Peninsula, determining the dimensions of the Wendeng granite body, the spatial distribution of fractures, deep geothermal temperatures, and the geothermal gradient. Zhang SS et al. (2019) explored HDR in the Gonghe Basin, drilling four HDR boreholes at depths of 2927–3705 m; they discovered a high-temperature rock body (>200°C at 3705 m), marking China's first HDR breakthrough in a non-modern volcanic area. Gao J et al. (2020) identified volcanic magma capsules and analyzed HDR formation conditions in the Wudalianchi Volcanic Group, confirming a volcanic magma capsule at a depth of 6.5 km in the Weishan area, indicating ideal geothermal conditions. Tan XF et al. (2020) explored HDR in the Chenzhuang uplift of the Jiyang Depression by conducting hydraulic fracturing tests on impermeable granite and dioritic granite layers at a depth of 2003–2500 m, and they recommended the use of natural fracture networks. Qi XF et al. (2020) and Li X et al. (2022) surveyed the Matouying uplift and discovered a high-temperature rock body (>150°C) at 3965 m.

Given HDR's inherently low natural permeability, its exploitation requires EGSs, which are artificial geothermal reservoirs created to extract thermal energy from low-permeability and low-porosity HDR. EGSs have emerged as a promising sustainable energy solution worldwide. The United States' Frontier Observatory for Research in Geothermal Energy initiative in Utah has advanced EGS technologies, particularly in reservoir creation and management (Moore J et al., 2019). The Habanero project in Australia, managed by Geodynamics, has demonstrated EGS viability through supercritical fluid production at high temperatures (Xu TF et al., 2022). In Europe, the Soultz-sous-Forêts project in France has pioneered continuous power generation from deep geothermal reservoirs (Koelbel T and Genter A, 2017). China's Gonghe Basin HDR Power Generation Demonstration project has shown significant potential, employing advanced drilling techniques to access high-temperature resources (Zhang EY et al., 2022). These examples demonstrate EGS development progress, highlighting advancements in reservoir stimulation, fluid circulation, and energy extraction methodologies essential for addressing geological challenges and improving geothermal energy production efficiency.

China's HDR exploration and EGS development are still in the early stages, focusing mainly on target site selection and deep geothermal resource assessment, with only a few experimental power generation projects underway. This paper presents a comprehensive review of recent advances in HDR exploration and EGS construction in China, examining geological conditions, genesis types, resource potentials, exploration findings, and EGS implementation. Additionally, it analyzes current challenges to guide future HDR exploration, development, and utilization in China and other regions.

2. Background and resource potential of HDR

2.1. HDR resource base

The HDR geothermal resource quantity is determined by

rock temperature and thermal properties, with the total resource base Q representing heat stored in low-porosity rock media, excluding fluid-stored heat. Assessing the HDR resource base is crucial for informing national and regional energy policy decisions and identifying development targets. In 2006, MIT published a landmark report titled "The Future of Geothermal Energy: The Impact of Enhanced Geothermal Systems on the U.S. in the 21st Century" (Tester JW et al., 2006), presenting the first systematic evaluation of HDR geothermal resources in the U.S. mainland and revealing significant resource potential. In 2011, the China Geological Survey (CGS) conducted initial assessments of China's HDR geothermal resource potential. Using the 2000 Chinese Heat Flow Distribution data (Hu SB et al., 2000) along with supplementary geothermal measurements, they estimated subsurface temperatures at various depths across China's land area (Fig. 1). The assessment indicated that HDR resources at a depth of 3.0–10 km in Chinese territory (including Taiwan) totaled 2.52 × 10^7 EJ (Lin WJ et al., 2012). Subsequently, Jiang GZ et al. (2016) performed a reassessment using updated heat flow data and comprehensive rock thermophysical properties and estimated mainland China's HDR resource base (excluding Taiwan) to be 2.29 × 10^7 EJ. Furthermore, they identified favorable HDR development zones in southern Xizang, western Yunnan (Tengchong), the southeastern coast, northern China, the Fenwei Graben at the southeastern edge of the Ordos Basin, and northeastern China (Songliao Basin). A comparison of the two HDR geothermal resource base assessments (Fig. 2), despite differences in the inclusion of Taiwan, shows that China's estimated HDR resource base remains consistent and exceeds the U.S. estimate of 1.67 × 10^7 EJ (excluding the Yellowstone area, Tester JW et al., 2006).

2.2. Types of HDR

Volcanic geothermal systems typically feature high-temperature thermal backgrounds, facilitating the presence of HDR resources in their vicinity. China, characterized by medium to low-temperature nonvolcanic geothermal systems and lacking modern volcanic eruptions, requires alternative approaches for HDR detection. Li DW and Wang YX (2015) developed a comprehensive geothermal energy classification system based on the thermal-tectonic characteristics of continental basin–mountain systems. This system categorizes geothermal energy into five types: plasma-thermal, dry-thermal, hydrothermal, aerothermal, and hybrid. They recommended concentrating HDR research on specific thermotectonic units, including thermally active composite orogenic belts, basins, land margins, and island arcs. Kong YL et al. (2021) examined upper crustal temperature heat sources and classified them into two categories with five subcategories: crustal-source (partially molten, non-magma-generated tectonic events, and radiative heat production) and mantle-source heat (magma and heat conducted from the mantle). Their review of global EGS projects revealed that

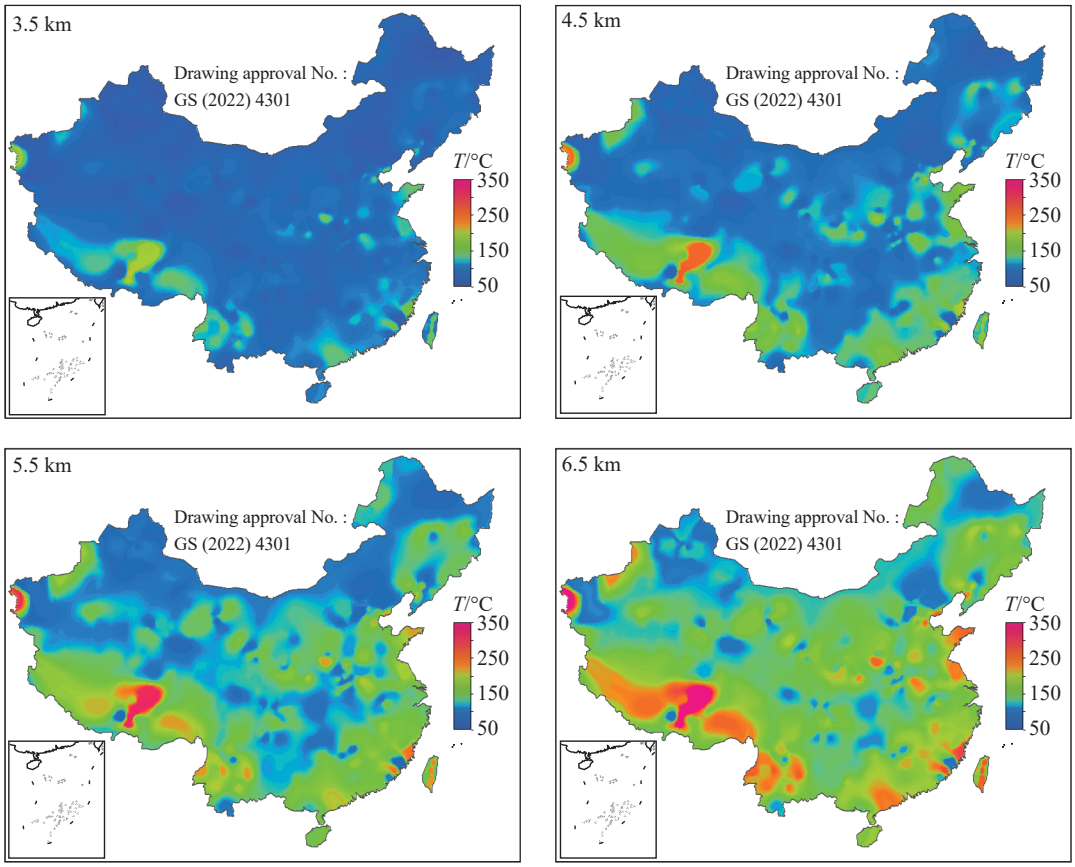

Fig. 1. Temperature distribution at a depth of 3.5–6.5 km in China's land area (after Lin WJ et al., 2012).

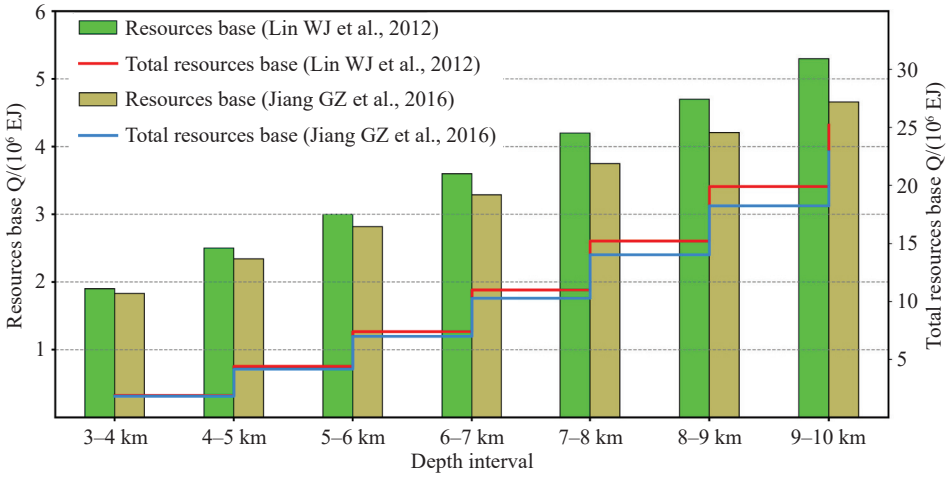

Fig. 2. Base resources of HDR at depths ranging from 3 km to 10 km in China's land area.

71% of these projects use mantle-source heat and suggested that future EGS exploration should prioritize areas with high heat flux (>100 mW/m^2). Wang GL et al. (2016), considering China's geotectonic context and relative scarcity of active volcanoes, identified four HDR resource genesis types: highly radioactive heat-producing, sedimentary basin, active volcanic, and intense tectonic activity zones (Fig. 3). The high-radiogenic HDR predominantly occurs in southeastern China's granite-rich regions, while sedimentary basin-type HDR is primarily found in eastern China, including the Songliao, North China, and North Jiangsu Basins. The basins' deep structural patterns facilitate heat flow redistribution, concentrating heat in deep basin uplifts. Active volcanic-type HDR exists mainly in Tengchong, Leiqiong, and Changbaishan, with heat characteristics closely linked to deep magmatism. The HDR in the strong tectonic activity zone is related to the uplift of the Qinghai-Xizang Plateau and intracrustal melting. The Indian-Eurasian plate collision resulted in crustal shortening and thickening, generating deep-melting magma sources, middle-crustal melting layers, and shallow magma intrusions, providing heat sources for HDR formation on the Qinghai-Xizang Plateau.

2.3. HDR heat source mechanisms

Recent drilling activities in high-temperature rocks and hydrothermal systems across the Gonghe Basin of Qinghai Province, the Matouying uplift of the North China Basin, and the Datong Volcanic Group have prompted extensive research into regional heat source mechanisms. Sun ZX et al. (2011) and Yan WD (2015) investigated the Gonghe Basin's high geothermal temperature sources. Sun ZX et al. (2011) identified deep granite bodies as the main cause of the region's elevated geothermal fields and abnormal geothermal gradients, indicating that HDR resources are likely to form in areas with favorable tectonic conditions. Yan WD (2015) used geophysical exploration data to propose that a high-temperature, low-velocity crustal layer potentially constitutes the regional HDR heat source, though this analysis remains qualitative. Zhang C et al. (2018) evaluated crustal and mantle heat production contributions in the Qiaboqia Valley using borehole logging and rock heat production data, and they established a "hot crust-warm mantle" crustal heat structure model for the Gonghe Basin. The current theory suggests that the Qinghai-Xizang Plateau's thickened crust contains a "low-velocity layer" providing crucial constant heat for HDR resource formation in the Gonghe Basin. Additionally, crustal thickening redistributes the radiogenic heat layer, serving as an important supplementary heat source for the basin's HDR resources (Lin WJ et al., 2021).

Significant debate exists regarding the presence of economically viable HDR resources in South China, with numerous analyses examining potential deep heat sources in the region. Wan TF et al. (1988) and Liao ZJ (2012) determined from Fujian's plate tectonic background that the upper crust lacks magmatic heat sources and conditions necessary for HDR power generation development. However, Teng JW et al. (2017) concluded that the southeast coast, located in the convergence zone of the Pacific and Eurasian plates—characterized by collision, extrusion, subduction, and subsidence—contains a low-velocity layer in the upper crust, indicating the presence of high-temperature geothermal reservoirs at depth. Studies by Zhao P et al. (1995) confirmed that granitic bodies in South China exhibit significantly higher radiogenic heat generation rates than global granite averages. Zhou ZM et al. (2020) analyzed the temperature field in South China and concluded that Mesozoic highly radiogenic heat-generating granitic bodies constitute the primary heat source contributing to the internal temperature of the crust. Studies by Mao XM et al. (2013), Tian J et al. (2021), and Wang S et al. (2022) analyzed helium, carbon isotopes, and noble gas compositions of geothermal water in South China and determined that deep fractures facilitate mantle communication and material upwelling, potentially serving as the primary energy source for certain hot springs. Based on HDR exploration borehole logging data and radiogenic heat generation data from major granite bodies in South China, Lin WJ et al. (2022) and Wang GL et al. (2023a, b) identified the granite body radiogenic heat generation rate, fracture structure, and capping conditions as principal factors

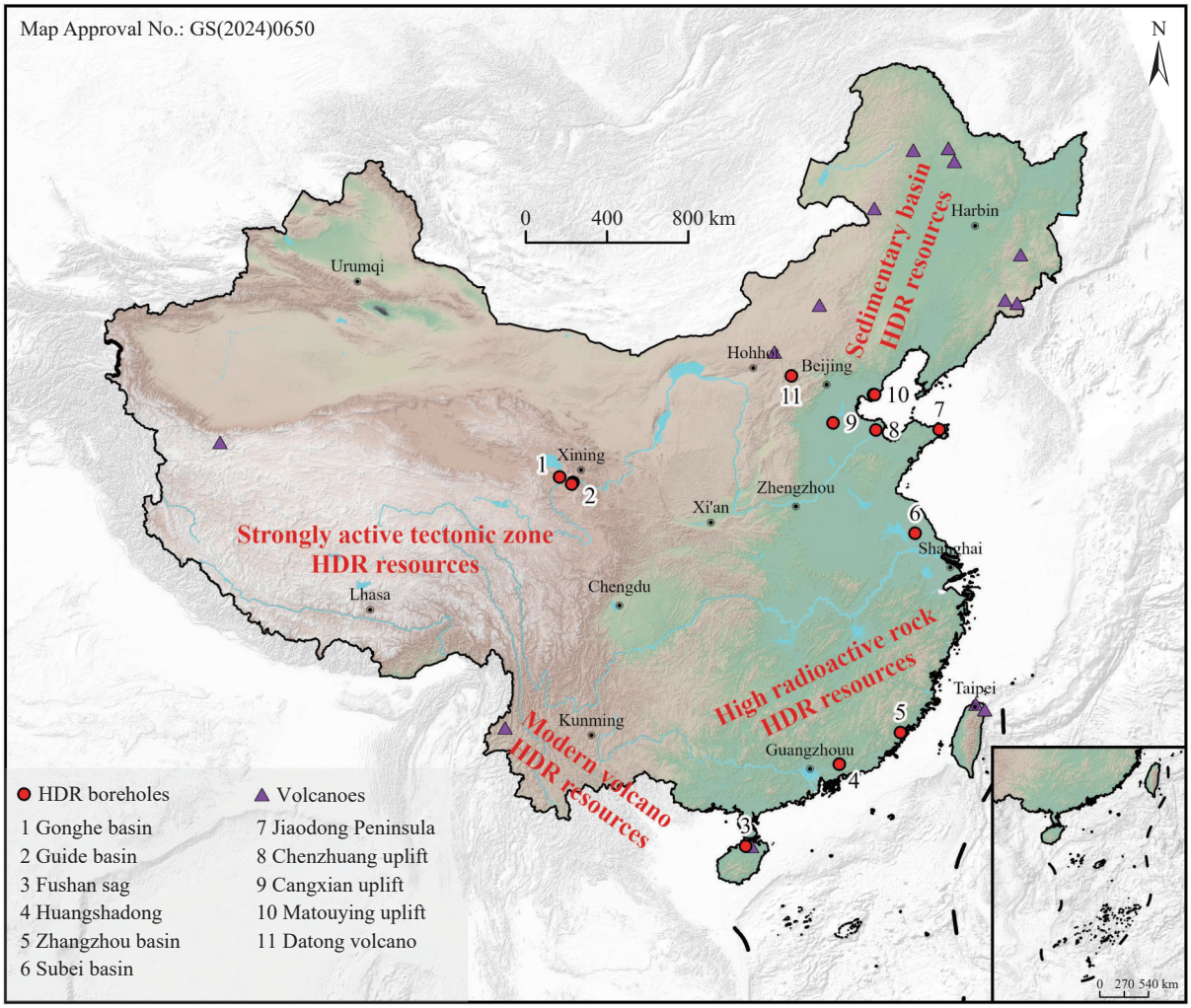

Fig. 3. Distribution of HDR resource types and exploration holes in China; the yellow dots represent the HDR exploration work conducted in China in recent years, and the list shows the geologic units or regions where they are located.

influencing the area's shallow geothermal field. Currently, except for the Fushan Depression oil field in Hainan, where rock layers with temperatures exceeding 185°C have been encountered (Cao R et al., 2022), HDR surveys in other South China regions have not yielded significant breakthroughs. The heat source model for HDR resources requires additional verification.

Researchers have conducted extensive analyses on the heat-gathering mechanism of hidden paleo-subduction mountains within sedimentary basins. Chen MX et al. (1990) systematically examined shallow geothermal field distributions in the North China Basin and identified bedrock undulation, tectonic morphology, groundwater activity, and magmatism as primary factors affecting shallow temperature distribution. Mao XP et al. (2018) and Wang XW et al. (2022) conducted geothermal field simulations for the Niutuozhen and Xianxian uplifts, respectively, and confirmed non-uniform near-surface heat transfer capacity as the determining factor in regional differential geothermal fields. Yin XX et al. (2021, 2024) analyzed geothermal dynamics monitoring data and tracer experiment results at the Cangxian uplift's northern end and suggested that basal fractures serving as heat flow channels influence the hydrothermal dynamic conditions of various geothermal reservoirs within specific ranges. Recent drilling discoveries of high-temperature rocks (>150°C) at a depth of 3965 m in the Matouying uplift further validate the heat-gathering mechanism in sedimentary basin paleo-subduction mountains, providing direction for HDR resource exploration. Qi XF et al. (2020) analyzed the Matouying uplift's geological structure and determined that the Baigezhuang Fault represents a regional fault penetrating the upper mantle, with upward heat transport along the fault providing additional thermal energy. Lin WJ et al. (2022) quantitatively evaluated fault heat contribution using crust-mantle heat flow data derived from HDR exploration hole logging and core radiogenic heat generation measurements.

3. HDR exploration progress

3.1. HDR exploration in sedimentary basins

The North China Basin is a Mesozoic–Cenozoic faulted basin that developed on the Sino-Korean Platform after Paleozoic sedimentation, shaped by tectonic activity during

the Indo-Chinese and Yanshan Period movements. The basin contains Paleozoic and Mesozoic strata overlain by substantial Cenozoic deposits (Yao YH et al., 2025). The basin comprises several primary tectonic structures, including the Jizhong Depression, Huanghua Depression, Jiyang Depression, Linqing Depression, Cangxian Uplift, and Chengning Uplift (Fig. 4b), forming a regional pattern of alternating elevated and depressed configurations. Extensive fractures separate the depressions and uplifts, with depression depths reaching several kilometers, creating favorable geological conditions for underground thermal water formation and storage. The basin's underground thermal water primarily occurs in two types of reservoirs: Paleocene and Neocene sandstone fissure-porosity geothermal reservoirs, and Paleocene and Paleozoic carbonate fissure-karst geothermal reservoirs. The carbonate fissure-karst geothermal reservoirs are predominantly situated in the basin's uplift areas. Recent HDR surveys conducted in Hebei and Shandong provinces have established multiple drill holes in the basin's uplift areas (Fig. 4b) and identified high-temperature rock bodies (>150°C) at 4500 m depth in the Matouying uplift. In this area, geothermal reservoir stimulation, connectivity testing, and power generation experiments have been implemented.

3.1.1. Matouying uplift in the North China Basin

The Matouying uplift is situated in the northeastern North China Basin, at the intersection of the Yanshan Fault Zone of the Sino-Korean quasi-terraneous plateau and the North China Fault, within a low plains area characterized by significant tectonic subsidence. This uplift represents a prominent secondary positive tectonic structure within the Huanghua Plateau Depression, bounded by the Mabei Fault to the north connecting to the Leting Depression, the Baigezhuang Fault to the west, and the Hongfangzi Fault to the south adjoining the Shijiutuo Depression. Seismic, gravity, and magnetic exploration data indicate that the Baigezhuang Fault represents a regional deep fracture extending into the upper mantle, potentially serving as a conduit for mantle heat flow. The oil exploration well Nan70-1, situated at the intersection of the Mabei and Baigezhuang faults, reached a depth of 1465 m and encountered aeolian granite at 1350 m. Temperature measurements revealed a temperature of 109°C at 1377 m, with the sedimentary cover exhibiting a substantial geothermal gradient of 7.2°C/100 m (Qi XF et al., 2020), indicating favorable geothermal conditions.

In 2018, the Hebei Coalfield Geological Bureau completed an HDR exploration borehole (M-1) in the Matouying uplift, reaching a depth of 4502.11 m (Fig. 4c).

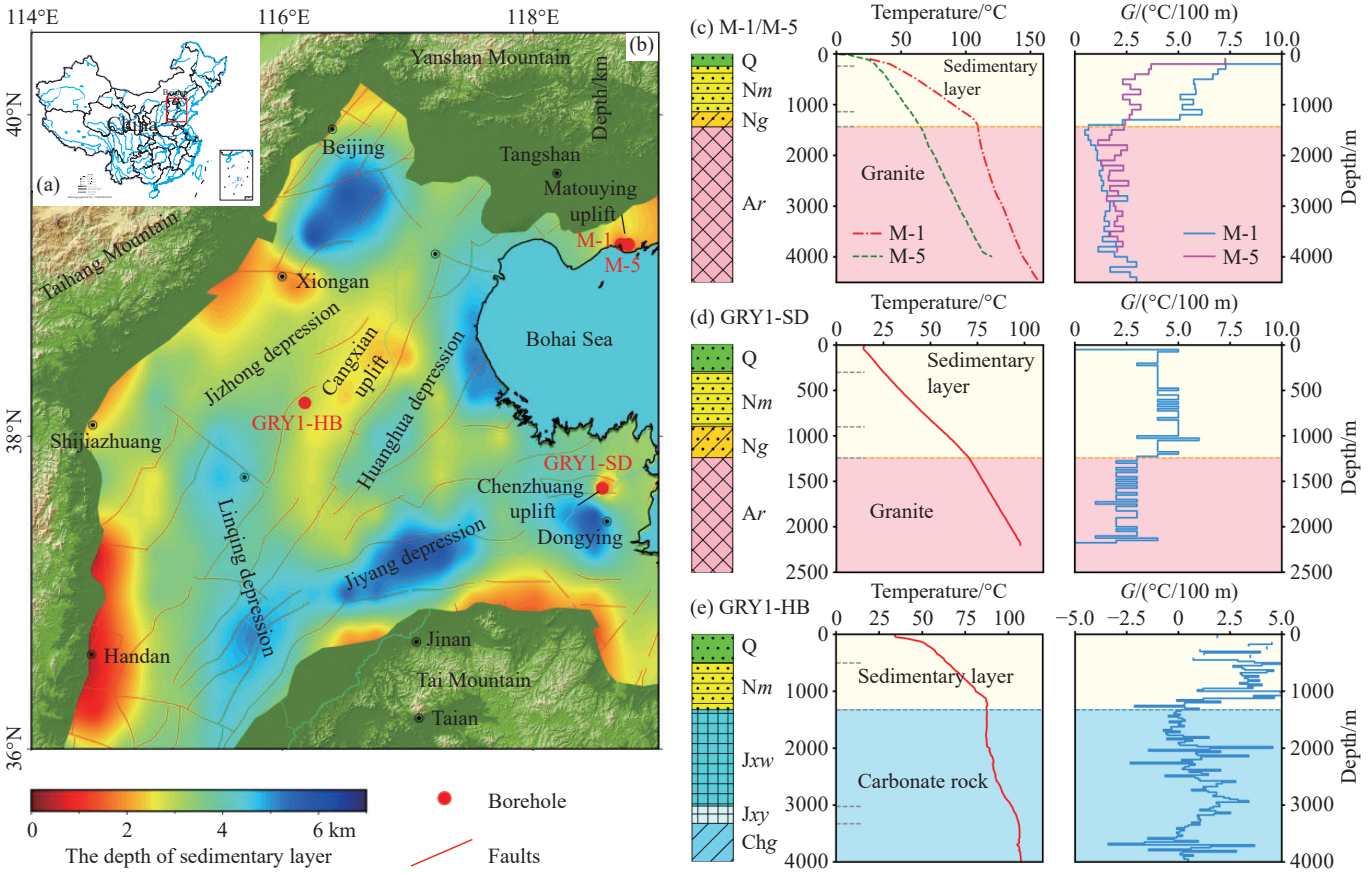

Fig. 4. Sediment thickness and distribution of HDR exploration boreholes in the North China Basin (sediment thickness data from CRUST 1.0, Laske G et al., 2013). The temperatures of the granites drilled at depth are notably higher than those of carbonate at depth, with the gradient exhibiting conductive warming characteristics. Q–Quaternary; N*m*–Minghuazhen Formation of the Neoproterozoic; N*g*–Guantao Formation of the Neoproterozoic; J*xw*–Wumushan Formation of the Jixian System; J*xy*–Yangzhuang Formation of the Jixian System; Chg–Gaoyuhuang Formation of the Changcheng System; and Ar–Archeozoic.

The borehole encountered an Archeozoic metamorphic rock series at 1376 m depth. Between 1400 m and 2600 m, the lithology primarily consists of metamorphic granodiorite and metamorphic quartz diorite, while diorite granite dominates below 2600 m. Logging data (Fig. 4c) indicate that M-1's bottom temperature reaches 157°C, with varying temperature gradients: 5–7°C/100 m in the Neogene cover; 1.2°C/100 m from the Neogene bottom to 2500 m; 1.7°C/100 m from 2500 to 3500 m; and 2.7°C/100 m below 3500 m. The bedrock exhibits a general trend of increasing geothermal gradient with depth. In 2021, borehole M-5 was drilled 5 km east of M-1 (Fig. 4b) along the Matouying uplift axis, reaching a depth of 4000.5 m, though recording a lower bottom temperature of 120.32°C (Fig. 4c).

3.1.2. Chengzhuang uplift in the North China Basin

The Chenzhuang uplift is situated in the southeast of the North China Basin, bordered by the Zhanhua Depression to the north and west, and the Dongying Depression to the south and east. The uplift exhibits a rectangular configuration, extending 23 km east to west and 5 km north to south, encompassing approximately 70 km^2. The Neoproterozoic and Quaternary cover thickness varies between 950 and 1200 m, with the uplift comprising metamorphic diorite of metamorphosed and Paleoproterozoic stratigraphic layers from the Paleoproterozoic era. In 2013, Shandong Province established an HDR exploration borehole —GRY1-SD —in the region (Fig. 4b); drilling commenced in June 2013 and reached completion in February 2014, at a final depth of 2500.58 m. GRY1-SD encountered the Neotethysian Taishan rock group at 1243.00 m, featuring basalt and minor intrusive granite in the upper section and metamorphic rocks including felsic gabbro and intrusive granite in the lower section. The logging data (Fig. 4d) indicate a temperature of 104.2°C at 2492 m depth, with an average geothermal gradient of 3.71°C/100 m. The temperature curve comprises two distinct sections: the cap section (0–1200 m) with an average geothermal gradient of 4.77°C/100 m, and the bedrock section, where the gradient decreases substantially to an average of 2.90°C/100 m (Tan XF et al., 2020). Both sections display linear temperature-depth curves, indicating typical conductive geothermal warming.

GRY1-SD underwent two hydraulic stimulation tests in 2014 (Tan XF et al., 2020). The primary fracturing occurred in two segments at 2180–2263 m and 2313–2411 m, where natural fractures were prevalent in a lithology comprising granite and diorite. The initial stimulation test resulted in pressure reduction for over 2 hours, with fracture closure following pressure decrease due to the absence of proppant support. During the second stimulation test, pre-rupture pressure (26.5 MPa) showed a 15% pressure reduction with consistent water injection, while post-rupture pressure demonstrated a 15% increase under the same injection conditions. These findings provide valuable insights for HDR resource development in this region.

3.1.3. Cangxian uplift in the North China Basin

The Cangxian uplift is positioned in the east-central region of the North China Basin and is geologically part of the broader Cangxian structural uplift (Long XT et al., 2023) (Fig. 4b). In 2016, the Hebei Coalfield Geological Bureau initiated an HDR exploration borehole (GRY1-HB) in the area. Drilling operations commenced on November 7, 2016, and concluded on May 20, 2017, reaching a depth of 4025.82 m (Fig. 4e). The stratigraphic sequence, from oldest to newest, is as follows: the Changcheng System Gaoyuzhuang Formation (Chg), partially exposed with a thickness of 258.36 m; the Jixian System Yangzhuang Formation (J*xy*), extending to 3767.46 m depth, with a thickness of 744.39 m; the Jixian System Wumushan Formation (J*xw*), reaching 3023.07 m depth with a thickness of 1696.47 m; the Neoproterozoic (N) unit, extending to 1326.60 m depth with a thickness of 822.64 m; and Quaternary (Q) deposits, reaching a depth of 503.96 m with a thickness of 503.96 m. The well maintained a bare borehole configuration after penetrating the Gaoyuzhuang Formation, with a bottom temperature of 107.5°C and wellhead water temperature of 103°C.

Following well completion, three logging operations were conducted, which revealed significant variations in geothermal gradients across different layers. The upper section (1326.60 m) comprises the Cenozoic cap section and exhibits a linear temperature-depth curve (Fig. 4d) characteristic of conduction-type warming, with the highest average gradient of approximately 3.5°C/100 m. Below this, in the bedrock section containing the carbonate geothermal reservoir, heat transfer primarily occurs through convection, with the gradient notably decreasing to an average below 1°C/100 m. Furthermore, due to limited stagnation time, drilling disturbances in the lower karst reservoir resulted in a more uniform temperature distribution.

A hydraulic stimulation test was conducted on the 3700–4000 m bare hole section of GRY1-HB from June 26 to July 16, 2017, spanning 21 days. Post-stimulation pumping tests revealed significant improvements: the water level increased from −43.74 m to −25.33 m, representing a 42% increase. The unit water influx increased from 0.8359 l/s.m to 1.7108 l/s.m, representing a 105% increase, demonstrating remarkable reservoir stimulation effectiveness. Subsequently, a scientific research facility was established for comprehensive geothermal resource development, focusing on medium- and low-temperature power generation and cascade utilization studies (Qin XX et al., 2019).

3.2. HDR exploration in areas with highly radioactive granite

The thermal potential of regional magmatic intrusions has received substantial attention. South China represents the country's most significant granite distribution area, with granite exhibiting exceptionally high heat generation rates (Zhao P et al., 1995; Lin WJ et al., 2024), creating favorable conditions for HDR formation. The CGS has conducted HDR resource exploration in Fujian and Guangdong provinces

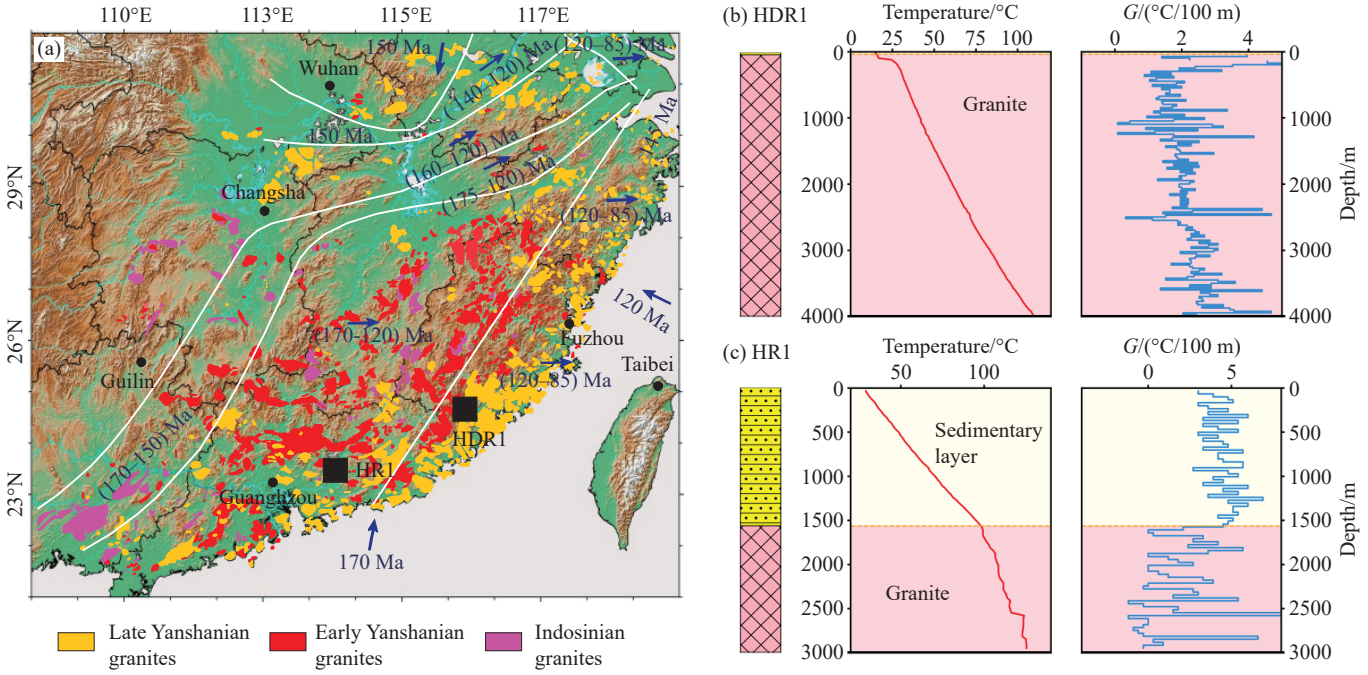

Fig. 5. Distribution of granites of different ages and deep drilling logging curves for HDR exploration in South China, demonstrating that the presence or absence of sedimentary cover at the surface significantly influences the temperature at depth.

since 2015, establishing several exploration holes, including HDR1 and HR1 (Fig. 5a). While HDR resources remain undetected, these efforts contribute significantly to understanding geothermal resource genesis and primary heat-controlling factors in South China, guiding future exploration and development practices in the region.

3.2.1. Qingquan Forestry Farm in Zhangzhou City, Fujian Province

Zhangzhou is situated on the southeastern edge of the Asian continent, within the southeastern coastal geothermal zone, one of China's four major geothermal regions, and the area with the highest concentration of medium- to low-temperature hot springs (Liu CL et al., 2022). The zone features numerous Late Mesozoic volcano-intrusive mafic rocks, forming an integral component of the near-Pacific Ocean region's significant tectonic-magmatic belt. In 2015, the CGS initiated HDR scientific drilling of hole HDR-1 at the Qingquan Forest Farm in Zhangzhou (Fig. 5b). Drilling commenced on May 21, 2015, and concluded on December 26, 2016, reaching a final depth of 4000 m. HDR-1 penetrated a 36-meter-thick surface layer of quaternary clay before entering the granite body, predominantly composed of granite, granodiorite, and diorite.

Multiple logging operations after drilling completion measured a final bottom temperature of 109.58°C at 3997 m (Fig. 5b), yielding an average geothermal gradient of 2.20°C/hm for the entire hole. The average geothermal gradients across different depth intervals were 1.71°C/hm (500–1000 m), 1.80°C/hm (1000–1500 m), 2.05°C/hm (1500–2000 m), 2.15°C/hm (2000–2500 m), 2.37°C/hm (2500–3000 m), 2.45°C/hm (3000–3500 m), and 2.78°C/hm (3500–4000 m), exhibiting a gradual increase with depth.

3.2.2. Huangshadong geothermal field in Guangdong Province

The Huangshadong geothermal field is situated northeast of Huizhou City in eastern Guangdong Province, encompassing approximately 260 km^2, and is characterized by northeast- and northwest-oriented fractures. The field lies within the NE-SW-oriented Meixian-Huiyang argillic depositional zone, positioned between the northeast-oriented Heyuan deep fault zone and the Lianhuashan deep fault zone. In November 2017, the CGS initiated the drilling of hole HR1 in the geothermal field (Fig. 5a), reaching a final depth of 3009.17 m on September 30, 2018. The drilling encountered the following strata in ascending order: Quaternary (0–20 m), Cambrian (21–466 m), Aurignacian (467–1565 m), and Jurassic rocks (1566–3009.17 m). The hole penetrated the sedimentary cover at 1565 m depth, accessing the lower hidden granite body. The encountered lithologies, from top to bottom, comprise sandstone, chondritic shale, charcoal/chalky slate, tectonic breccia, silicified quartz sandstone, sericitized granite, and diorite. Following completion and brief pumping, continuous self-spraying occurred, achieving a maximum stable wellhead water temperature of 118°C and a maximum flow rate of 137 m^3/h.

Post-drilling, multiple geothermal logging operations were carried out. The final measured bottom temperature reached 127.7°C, with rapid increases observed in the 2400–2500 m and 2700–2800 m sections (Fig. 5c), indicating the main hot-water outflow sections. The geothermal gradient analysis revealed an average of 4.52°C/hm from 0 m to 1500 m, while the average gradient at the 1565 m section measured only 2.03°C/hm.

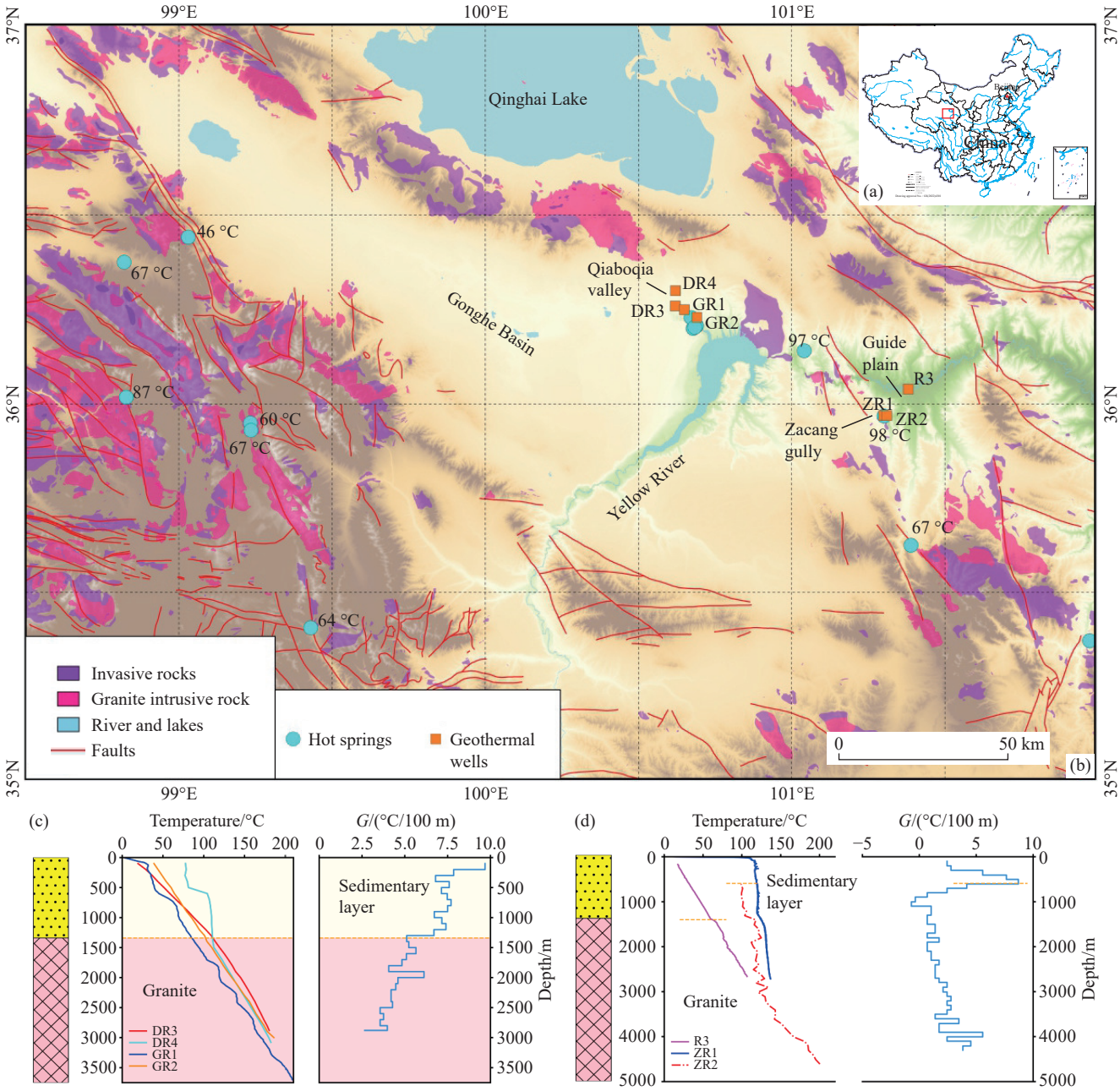

Fig. 6. Gonghe Basin in Qinghai Province exhibits significant geothermal characteristics, including multiple geothermal points and surrounding hot springs. The region demonstrates a high geothermal gradient, particularly in tectonic fissure areas where hot springs emerge (ZR2 in Fig. 6d). The deeper sections exhibit conductive heat transfer with elevated geothermal gradients, while the upper sections exhibit convective characteristics.

3.3. HDR exploration in tectonically active zones

The Gonghe Basin, situated on the northeastern margin of the Qinghai-Xizang Plateau, represents a diamond-shaped Cenozoic faulted basin with a northwesterly spread (Fig. 6), covering approximately 1.7×10^4 km^2. The northern margin is bounded by the Zongmulong-Qinghai Nanshan Fault, a super lithospheric active fault exhibiting a slightly southerly dipping near-erect profile. The southern boundary corresponds to the main margin of the Jingyuhu–Animachine Late Paleoproterozoic to Early Mesoproterozoic suture zone. This boundary is marked by a lithospheric or sub-lithospheric fault that generally dips steeply to the north. During the Cenozoic era, influenced by the Himalayan orogenic movement, the Gonghe Basin underwent intense neotectonic activity, evidenced by the resurrection of old fractures around and within the basin. Enhanced hydrothermal activity in the basin's deeper regions established favorable geological and tectonic conditions for geothermal resource formation (Zhang FS et al., 2023). Furthermore, the basin contains 600–2400 m thick fine-grained Quaternary alluvial strata and Neoproterozoic Pliocene mudstone strata, providing thermal insulation that maintains the basin's high geothermal background. Since 2011, multiple geothermal exploration holes have been drilled in the Gonghe Basin, with several detecting high-temperature rocks (>180°C), marking a significant advancement in China's

HDR exploration.

3.3.1. Qiaboqia Valley in the Gonghe Basin, Qinghai Province

Since 2011, Qinghai Province has implemented several geothermal water exploration projects in the Qiaboqia Valley of the Gonghe Basin to address urban heating needs. Multiple boreholes exceeding 2000 m in depth have been drilled (Fig. 6b), revealing a basin basement composed of Indosinian granite overlain by Quaternary (Q) and Neoproterozoic (N) strata with thicknesses ranging from 1300 m to 1500 m. The granite body beneath the basin remains largely intact. Two notable boreholes, DR3 and DR4, situated 4 km apart, encountered granite at depths of 1360 m and 1400 m, respectively. The DR3 borehole reaches 2927.26 m deep with a bottom temperature of 181.17°C, while DR4 extends to 3102.00 m with a bottom temperature of 175°C. Temperature logging curves (Fig. 6c) demonstrate linear temperature-depth relationships, indicating typical conductive characteristics. DR3 exhibits an average geothermal gradient of 5.99°C/100 m, with the sedimentary cover above 1360 m showing a higher gradient of 7.73°C/100 m, decreasing to 4.37°C/100 m within the granite body.

Since 2017, Qinghai Province has initiated HDR exploration in the Qiaboqia area, drilling exploration holes including GR1 and GR2 (Fig. 6b). The GR1 borehole extends to 3705 m, with Cenozoic sedimentary cover above 1350 m and Middle and Late Triassic granite from 1350 m to 3705 m. The primary lithological composition includes granitic syenite, (melanoclastite) granite, diabase granite, granodiorite, (black mica) granite, diorite, and porphyritic (black mica) diorite. Logging data (Fig. 6c) indicate an average geothermal gradient of 7.14°C/100 m in the 2500–3705 m section, with bottom hole temperatures reaching approximately 209°C.

3.3.2. Guide Plain in the Gonghe Basin, Qinghai Province

The Guide Plain, situated in the eastern Gonghe Basin, encompasses a geothermal anomaly area including the Guide Plain and Zacan Gully Geothermal Field at the basin's periphery (Fig. 6b). The gully features a canyon with steep terrain on its northern and southern flanks, where hot springs align linearly along the hot water gully. Approximately 30 springs emerge within a 100 m stretch, reaching temperatures up to 98°C, with associated H_2S gas emissions (Liu LX et al., 2024; Lu R et al., 2024).

In recent years, multiple deep hot water exploration boreholes have been drilled in the Guide Plain to investigate geothermal resources. The R3 borehole, reaching a depth of 2701.2 m, encountered deep granite at 1400 m with a bottom temperature of 103.74°C, indicating favorable geothermal conditions. Between 2013 and 2018, the HDR exploration boreholes ZR1 and ZR2 were drilled by the Qinghai Environmental Geological Survey Bureau in a hot water gully (Fig. 6b). The ZR1 borehole, extending to 3050.68 m, primarily encountered Indo-Chinese granodiorite and coarse-grained granite, with a bottom temperature of 151.34°C. Furthermore, the borehole encountered three distinct underground hot water aquifers with fracture zones at 50–600 m, 1200–1700 m, and 2200–2800 m, while relatively intact or water-isolated sections occurred at 600–1200 m and 1700–2200 m. The temperature and pressure remained relatively stable above 1200 m, at approximately 120°C, indicating stable geothermal fluid conditions. A significant temperature increase occurred between 1200 m and 1500 m, corresponding to intact core and water depletion zones. Below 1500 m, the ground temperature gradient stabilized with gradual temperature increases (Fig. 6d). The ZR2 borehole reached 4721.6 m, with Neoproterozoic mudstone cover at 592.07 m, followed by black mica diorite, quartz diorite, and granodiorite. At 4633 m, the measured temperature of 214°C represents China's highest recorded HDR temperature. The geothermal gradient varies as follows: 6.08°C/100 m (0–1650 m), 2.33°C/100 m (1650–3000 m), and 4.94°C/100 m (3000–4700 m), averaging 4.15°C/100 m. The gradient is lower in the upper mudstone and sandstone layers but increases notably in granite formations, stabilizing below 3000 m. The drilling has revealed the stratigraphy of a complete HDR geothermal system.

3.4. HDR exploration in active volcanic areas

3.4.1. Datong Volcanic Group, Shanxi Province

The Datong Basin, a Cenozoic fault basin, is situated where the central belt of the North China Massif intersects with the Inner Mongolia Suture Belt in the North China Craton. The North China Craton has experienced multiple tectonic movements since the Late Mesozoic, resulting in localized lithospheric modification and thinning. Quaternary volcanic activity in the Datong Basin, influenced by neotectonic movement, occurred in three distinct phases between 0.78 Ma and 0.1 Ma, spanning from the late Early Pleistocene to early Late Pleistocene. Lithospheric thinning, driven by extensional and tensile stresses, enabled asthenospheric magma to rise, triggering partial melting of upper mantle material. This magma then erupted through deep faults and weakened zones, leading to the formation of the distinctive Datong Volcanic Group (Zhou WL et al., 2022). While volcanic formations predominantly occur around the basin's perimeter and the southern region near deep faults, the Yanggao-Tianzhen area in the northeastern basin shows limited volcanic exposure, suggesting potential deep magma intrusion zones with magma capsules or high-temperature anomalies.

The Yanggao-Tianzhen Basin, a sub-basin situated in the northern portion of the Datong Basin, extends in the NEE direction (Fig. 7b). Geologically, it forms part of the Yanggao–Tianzhen block uplift within the Northern Margin Tectonic Belt of the North China Plate. In March 2020, the First Hydrogeological Geological Team of the Shanxi Geological Survey Bureau commenced HDR resource exploration in the Yanggao-Tianzhen Basin and drilled HDR exploration hole DR1 (Fig. 7b), which reached a depth of

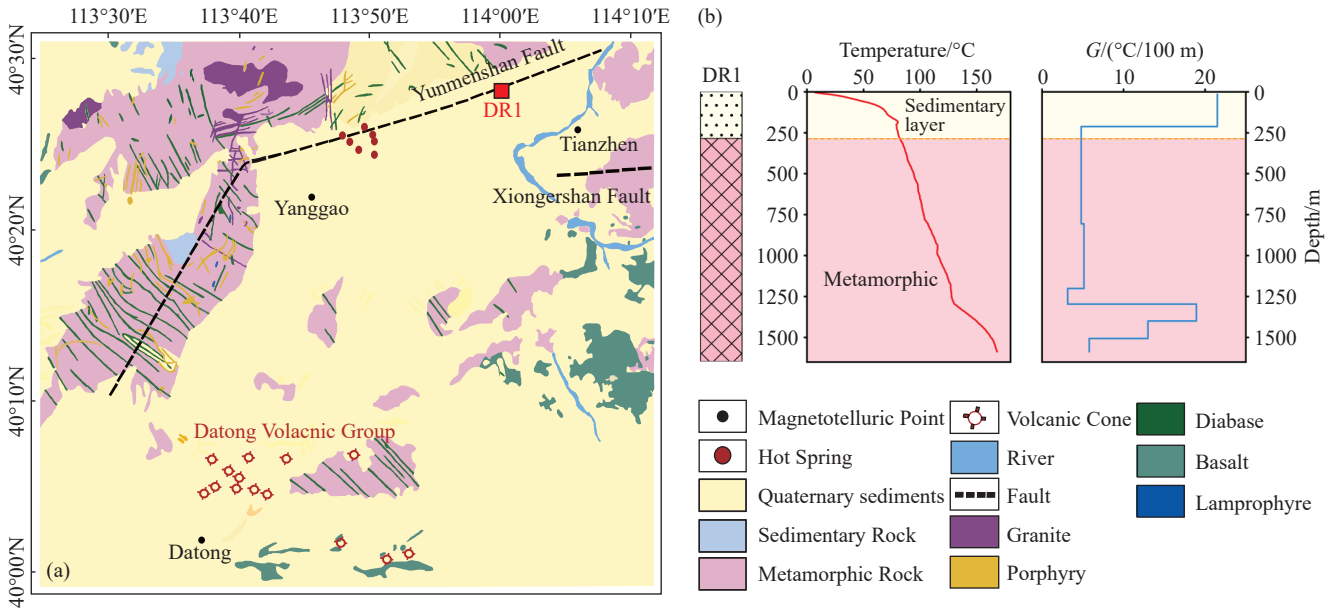

Fig. 7. Regional geologic sketch of the Datong Basin and logging curves of the HDR exploration hole (modified from Zhou WL et al., 2022).

1624.01 m. The hole penetrated the overlying sedimentary layer into the underlying metamorphic basement at 769 m, exposing Quaternary, Tertiary, and Neo-Palaeozoic strata. The sedimentary layers primarily consist of subclay, sandy soil, and gravel, while the metamorphic basement predominantly comprises black cloud dioritic gneiss. DR1 identified high-temperature and high-pressure geothermal fluid, with bottom temperatures reaching 167.94°C (Fig. 7c) and outlet water temperature reaching 160.2°C. Blowout test results indicated a wellhead pressure of 1.12 MPa, a maximum flow rate of 231.15 m^3/h, and an estimated annual usable thermal energy of 11.45 × 10^8 MJ per single well. DR1 achieved power generation with an installed capacity of 280 kW in early 2021.

3.4.2. Qiongbei Volcanic Group, Hainan Province

The Qiongbei region, situated at the southeastern edge of the Eurasian Plate, has been significantly affected by the Philippine Plate, Indian Plate, and South China Sea Basin expansion, resulting in intense tectonic movements, volcanism, and seismic activities. Surface Quaternary volcanic activity records indicate that the most recent and intense eruption occurred during the Holocene period, approximately 10,000 years ago. Seismodynamic analysis indicates that frequent and intense Quaternary volcanism likely created magma capsules within the region's deep crust, primarily contributing to local anomalous ground temperatures (Chen KQ et al., 2022). Additionally, the region features a Cenozoic fault rift basin, the Beibuwan Basin, developed on a pre-Palaeoproterozoic basement, whose extensive sedimentary layer provides thermal insulation for deep heat energy, essential for HDR resource formation.

The Leiqiong Basin represents the onshore portion of the Beibuwan Basin, encompassing the Leizhou Peninsula and northern Qiongbei, with the two regions separated by the Qiongzhou Strait. Recent petroleum exploration in the Leiqiong Basin has revealed high-temperature strata at depth, including the XU4 well in Xuwen County, which reached 3203.18 m with a temperature of 146.4°C measured at 3150 m. The well exhibited an average geothermal gradient of 3.44°C/100 m, with sections from 0 m to 1500 m averaging 2.88°C/100 m and 1500 m to 3200 m averaging 3.96°C/100 m. Additional oil boreholes in the Fushan Depression, west of Haikou City, encountered stratified geothermal gradients: lower values of 2.4–3.1°C/100 m in upper sections and higher values of 4.0–5.6°C/100 m in lower sections, with stratification boundaries varying between 2300 m and 3000 m (Zhao YD et al., 2016). On December 28, 2017, the HDR parameter well HD-1R, drilled by Bohai Drilling No.1 Drilling Company, reached high-temperature rocks (>185°C, non-steady state) at 4387 m depth after 66 days of drilling, discovering HDR resources in terrestrial sedimentary rocks south of the Leiqiong Rift Valley.

4. Progress in the construction of EGSs

4.1. EGS in the Gonghe Basin

In 2019, the CGS established a testing facility for HDR exploration and experimental development in the Gonghe Basin of Qinghai Province (Fig. 8). The initial HDR production test well, GH-01, was designed and drilled to a depth of 4000 m, achieving a bottom temperature of 207°C. Subsequently, reservoir stimulation tests were performed. To effectively monitor the deep fracture distribution, a comprehensive microseismic monitoring system was implemented, combining surface, deep, and shallow well measurements. In 2020, guided by the fracture distribution data from microseismic monitoring, two directional wells, GH-02 and GH-03, were designed and drilled. The three wells were aligned linearly, with GH-02 and GH-03 positioned 60 m on either side of GH-01, with boreholes at distances

Fig. 8. HDR exploration, experimental development, and generation test site in the Gonghe Basin, Qinghai Province.

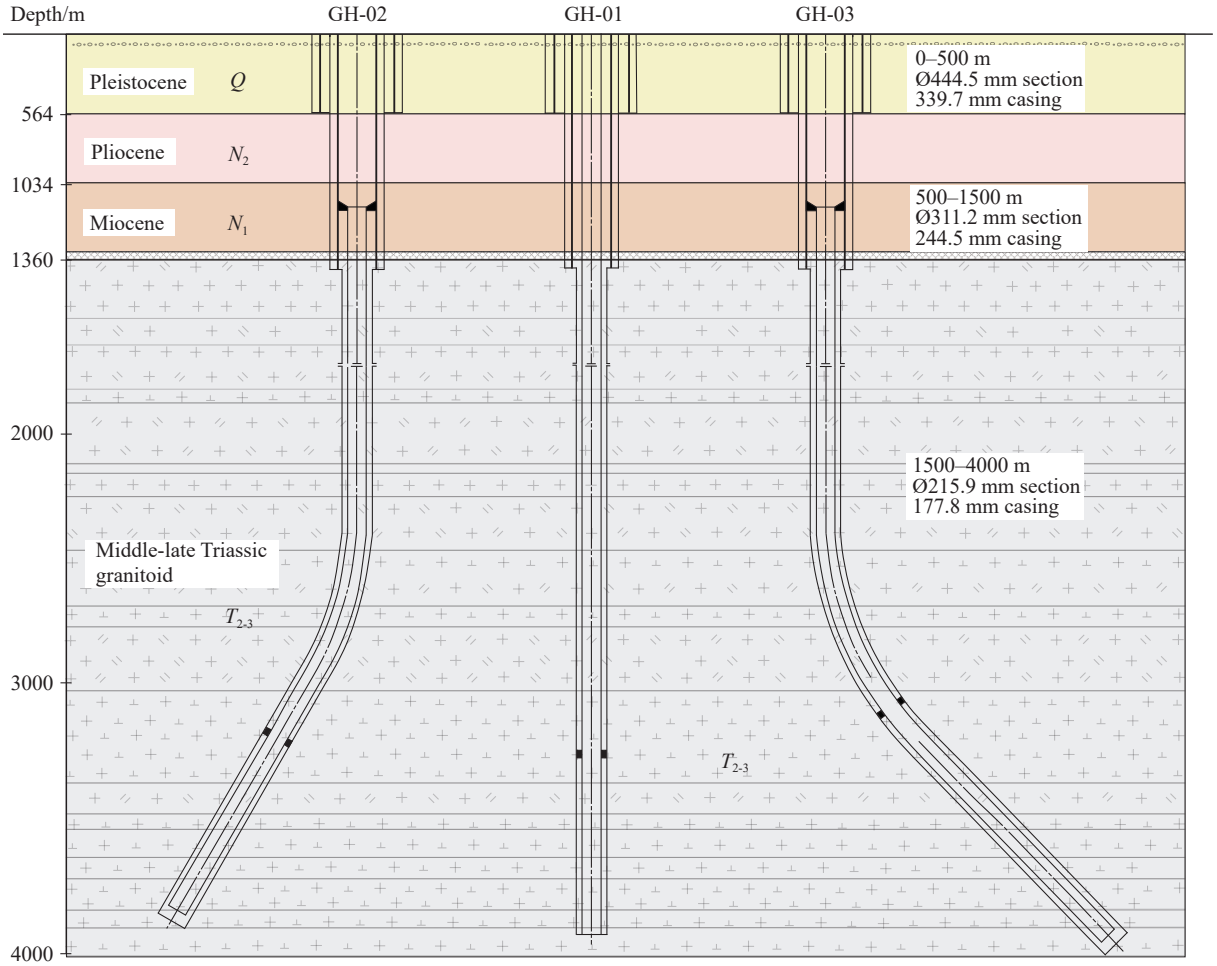

Fig. 9. Schematic of the HDR test well group in the Gonghe Basin (after Zhang EY et al., 2022).

ranging from 180 m to 380 m in the HDR reservoir. The completed HDR test well group comprised one vertical and two directional wells (Fig. 9).

The reservoir stimulation in this test well group proceeded through three distinct stages: minifrac test, fracturing pilot test, and large-scale stimulation (Zhang EY et al., 2022). The minifrac test was designed to evaluate the target reservoir's physical properties, fracturing fluid viability, and equipment suitability. During the 6-day minifrac test, the cumulative fluid injection volume reached 1491 m^3, with a maximum pumping rate of 2.5 m^3/min, a maximum wellhead pressure of 42.6 MPa, and an effective stimulated reservoir volume of 6×10^5 m^3. Subsequent analysis revealed that the in-situ reservoir permeability was approximately 2.6×10^{-2} mD. The fracturing pilot test primarily focused on technical preparation for large-scale production enhancement. HDR shear fracturing tests were conducted at varying pump speeds and fluid volumes to analyze fracture extension characteristics. This phase achieved a cumulative fluid injection volume of 4300 m^3, a maximum pump speed of 3.05 m^3/min, a maximum wellhead pressure of 48.1 MPa, and an effective stimulated reservoir volume of 2.41×10^6 m^3. Large-scale reservoir stimulation was implemented based on the minifrac and fracture pilot test results. To achieve effective HDR shear and fracture extension under low-energy microseismic events, the process used a low pumping rate of <3 m^3/min with continuous injection periods of 8–24 hours. Stepless variable speed fracturing equipment facilitated continuous pumping injection and soft well shut-in to minimize pressure shock effects. Large-scale fracturing was accomplished through shock-absorbing technology, optimized fracture extension processes, and multi-stage operations. The total fluid injection volume exceeded 2×10^4 m^3, with a maximum pumping rate of 3.05 m^3/min and a maximum wellhead pressure of 48.1 MPa (Fig. 10). The effective reservoir volume near GH-01 surpassed 1.2×10^7 m^3.

After completing geothermal reservoir stimulation tests, researchers carried out fluid circulation and inter-well connectivity testing (Zhang EY et al., 2022). Using a series of technical measures —such as alternating injection and extraction, acid injection and dissolution, and gun perforation —the inter-well circulation tests achieved flow rates ranging from 15.4 m^3/h to 22.5 m^3/h (Fig. 11). The temperature ranged from 110.4°C to 125.7°C, while the injection well pressure decreased from 65.3 MPa to 54.6 MPa.

In 2022, two additional test wells, GH-04 and GH-05,

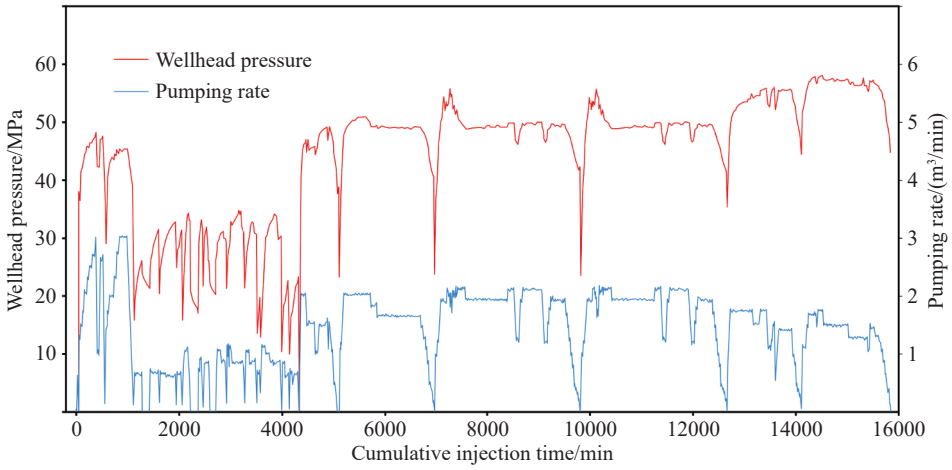

Fig. 10. Injection pressure and pumping rate during reservoir stimulation in the Gonghe Basin (after Zhang EY et al., 2022).

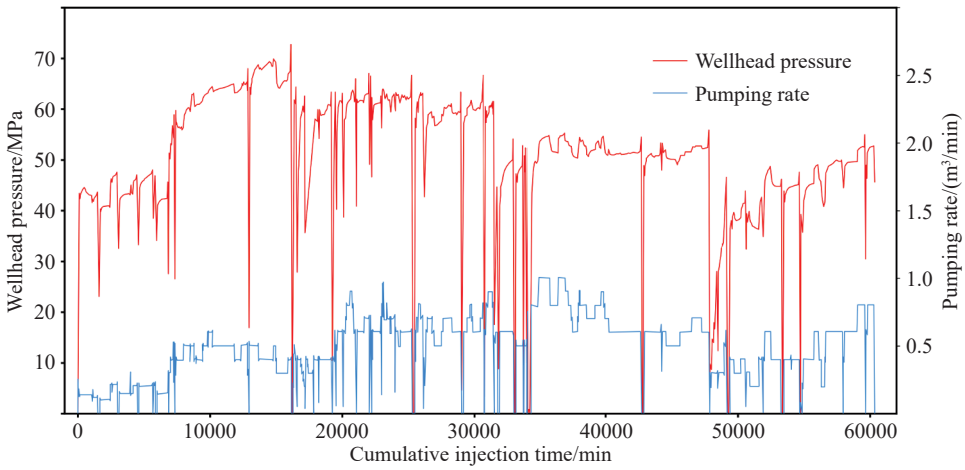

Fig. 11. Injection rate and pressure curves during circulation in the Gonghe Basin (after Zhang EY et al., 2022).

were drilled in this test site (Fig. 8) for ongoing circulation interconnect tests.

4.2. EGS in the Matouying uplift

The test well group in the Matouying uplift of the North China Basin comprises wells M-1 and M-2, with a depth of 4500 m, a spacing of 200 m, and a target stimulated reservoir section of 4200–4500 m (Fig. 12). The Bureau of Coalfield Geology of Hebei Province conducted the M-1 stimulation test from December 10 to December 19, 2020. The stimulation process involved initial small-scale pumping, followed by medium-scale pumping and large-scale pumping. During the pre-fracturing stage, a low flow rate of 3.5 m^3/min was used for fracture expansion, while a flow rate of 4.0–5.5 m^3/min facilitated reservoir longitudinal communication in the middle stage. In the later stage, a flow rate of 6 m^3/min was used to further promote the rapid expansion of the previously opened fractures. To enhance tension-shear mixing rupture effects, 13 m^3 ceramic proppant was introduced to maintain seepage through the tensile fracture after closure. The operation spanned 10 days, using 15224 m^3 of fracturing fluid (approximately 255 m^3 of fresh water and 14969 m^3 of slickwater) and 12.75 m^3 of proppant, achieving a maximum pressure of 65 MPa and a maximum flow rate of 6.05 m^3/min. A subsequent reservoir stimulation test was performed in the M-2 well from May 14 to 21, 2021, injecting 16145.5 m^3 of fluid and 10.1 m^3 of proppant and achieving a maximum flow rate of 7.03 m^3/min. The total fracturing fluid injected into the M-1 and M-2 wells amounted to 31369.5 m^3, resulting in 3029 rupture events. Of these events, 2575 were tensile ruptures, 242 were shear ruptures, and 212 were mixed ruptures, with shear and mixed ruptures constituting 15% of the total rupture events.

The reservoir cycling test commenced on June 24, 2021. The injection process of the M-1 well comprised two distinct stages, with initial average injection flow rates of 50 m^3/h and subsequent rates of 70 m^3/h. Under the 70 m^3/h injection condition of the M-1 well, the self-flowing rate of M-2 surpassed 20 m^3/h. The produced flow temperature increased rapidly from 30°C to 70°C shortly after well opening, followed by a gradual deceleration before stabilizing at approximately 108°C during the final testing phase.

5. Discussion

5.1. Carbon emission reduction potential of HDR resources

The assessment of carbon reduction potential through the replacement of coal-fired power generation with HDR in

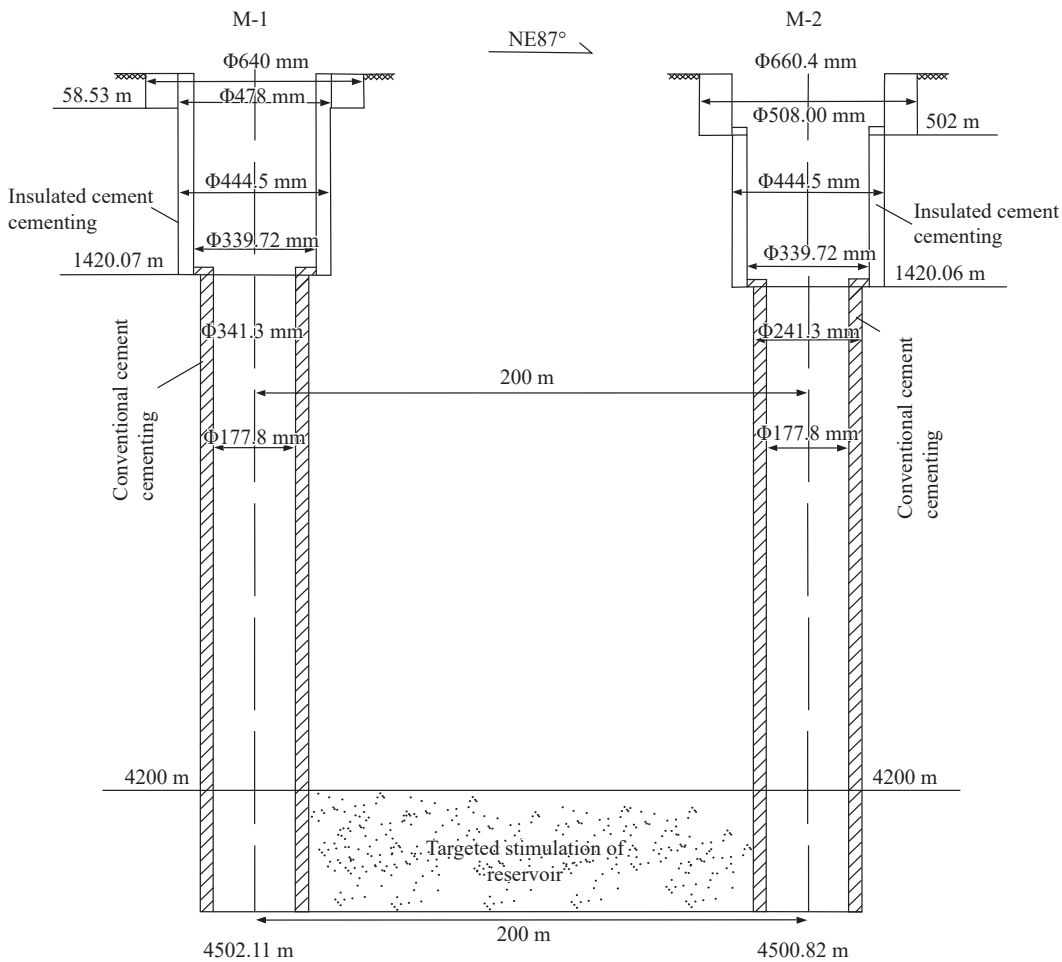

Fig. 12. Schematic of the hot dry rock test well group in the Matouying uplift, North China Basin.

China uses the "Baseline Scenario Comparison Method." This analysis encompasses the following: (1) HDR resource and power generation capacity conversion; (2) a comparison between baseline carbon emissions from coal-fired power generation and HDR life cycle emissions; and (3) sensitivity analysis.

5.1.1. HDR resources and power generation capacity

The total HDR thermal energy at depths of 3–10 km in China's land area amounts to 2.5 × 10^{25} J (Lin WJ et al., 2012; Wang L and Jia LQ, 2024). Based on the technically extractable rate of 2%, the total usable thermal energy ($E_{extractable}$) approximates 5 × 10^{23} J. With a thermoelectric conversion efficiency η = 12%, the power generation capacity (E_{elec}) is calculated as follows: E_{elec} = η·*extractable rate of 2%, the total usable thermal energy* ($E_{extractable}$)/3.6 × 10^6 J/kWh = 1.67 × 10^{16} kWh, equivalent to replacing 2.05 × 10^{12} tons of standard coal (assuming 35% coal power efficiency).

5.1.2. Comparative analysis of carbon emissions

A comparison between HDR full life cycle emissions and baseline scenario (coal power) emissions reveals significant differences. Using China's coal power emission factor of 0.85 kg CO_2/kWh (Wang N et al., 2018), the total equivalent electricity (E_{elec}) emission (C_{coal}) reaches 1.42 × 10^{16} kg CO_2. Research by Sigurjónsson HÆ et al. (2021) examining two deep EGSs' climate change impacts found emission factors of 1.6–17.4 gCO_2/kWh and 6.9–13.9 g CO_2/kWh for systems in Reykjavík, Iceland, and Vandenheim, France, respectively. Given China's nascent EGS development stage, applying an emission factor of 0.05 kg CO_2/kWh yields a total emission (C_{EGS}) of 8.35 × 10^{14} kg CO_2. This indicates China's HDR net emission reduction potential of 1.34 × 10^{16} kg CO_2, achieving a 94.4% emission reduction efficiency. Over a 100-year development cycle, this represents an average annual reduction of 1.34 × 10^{10} t CO_2, equivalent to 117% of China's 2022 carbon emissions.

5.1.3. Sensitivity analysis

The carbon reduction potential of HDR development is influenced by multiple factors, with key uncertainties primarily stemming from technological maturity, the geographic distribution of resources, power generation efficiency, and the capacity of the power grid to absorb output. Current EGS drilling and reservoir stimulation technologies are still under development, and deep drilling beyond 5 km remains costly and poses notable risks of induced seismicity. Should technological advancement lag, the actual recoverable rate might fall below 2%, substantially diminishing the emission reduction potential. Geographically, China's HDR resources are concentrated around the Qinghai-Xizang Plateau, distant from eastern high-load power centers. Transmission losses (approximately 5%–8%) over long distances and inadequate grid infrastructure may restrict resource utilization rates, potentially limiting the revised exploitable scale to 10%–30% of the theoretical values. HDR thermoelectric conversion efficiency (η) varies with reservoir temperature and circulating materials, with practical efficiency typically ranging between 10% and 15% (Zarrouk SJ and Moon H, 2014). A reduction in efficiency from 15% to 10% would decrease total power generation by 17%, resulting in emission reductions of approximately 1.8 × 10^{12} t CO_2. Furthermore, geothermal power generation's intermittent nature, necessary for reservoir pressure maintenance, may necessitate supplementary storage or peaking power facilities. Insufficient grid flexibility could lead to power abandonment, further diminishing emission reduction benefits. Considering these factors collectively (Table 1), under conservative estimates (1% recoverability, 10% efficiency, and 10% development ratio), annual emission reductions might achieve only 5%–10% of theoretical projections (approximately 1.34 × 10^9 of CO_2/year), emphasizing the importance of coordinated technology advancement and policy implementation.

5.2. HDR in varying geological settings

5.2.1. HDR within sedimentary basins

Sedimentary basins typically lack intracrustal anomalous heat sources (such as magma vesicles), and their internal depression-medium convexity structure creates variations in thermal conductivity along the horizontal direction, leading to changes in the temperature field (Wang GL et al., 2023c). When bedrock with high thermal conductivity exists beneath substantial sedimentary cover, heat flow from the standard basement concentrates toward the convex sections of the bedrock, resulting in more pronounced heat flow in uplift areas than in depression areas (Mao XP et al., 2018, 2019). This means that high thermal conductivity layers in the deep sedimentary basin can efficiently transfer basement heat to shallow regions, creating anomalously high temperatures. Consequently, uplift zones in deep sedimentary basins with effective thermal insulation represent optimal target areas for HDR exploration. The North China, Songliao, and North Jiangsu Basins in eastern China feature thick sedimentary sequences and multiple overlapping geothermal reservoirs, with heat flow values ranging from 60 mW/m^2 to 83 mW/m^2 (Qiu NS, 1998). These characteristics make them key target areas for the exploration and development of sedimentary basin-type HDR resources.

Recent HDR exploration in China has involved several boreholes being drilled in the bedrock uplift of the North

Table 1. Sensitivity analysis of HDR carbon reduction potential in China.

Parameters	Reference value	Range of variation	Range of fluctuations in emission reductions
Extractability/%	2	13	±50%
Power generation efficiency/%	12	10–15	±18%
Percentage of actual development/%	100	10–30 (practical constraints)	−90% to −70%

China Basin. While the M-1 well in the Matouying uplift encountered high-temperature rock (>157°C) at 4500 m depth, other wells showed less favorable temperatures. The M-5 well, located approximately 5 km from M-1, recorded only 120.32°C at 4000.5 m depth, indicating additional geological factors affecting the subsurface temperature field. Lin WJ et al. (2023) analyzed the geological conditions of the M-1 and M-5 wells and suggested that the M-1 well's thermal anomaly results from both normal upper mantle heat conduction and deep fractures connecting to mantle heat sources. Petroleum exploration data from the Matouying area reveal thick basalt deposits at specific depths associated with fractures, confirming that these deep fractures have significant heat conduction properties. The primary heat sources for HDR resources in the North China Basin stem from the high-temperature thermal background driven by local lithospheric thinning in the North China Craton and deep thermal material upwelling through fractures. Future HDR exploration in sedimentary basins must consider bedrock surface undulation, upper overburden thickness, and the presence of deep fractures connected to mantle heat sources.

5.2.2. HDR within highly radioactive granite

While metamorphic rocks (such as gneisses) and magmatic rocks (including granites and diorites) at certain crustal depths can theoretically serve as HDRs, granite formations with high temperatures account for the majority of currently developed HDR resources. Granite contains significant concentrations of radioactive elements, including U, Th, and K, whose decay heat represents a primary crustal heat source. Rybach L et al. (1978) calculated the heat generation rate per unit volume (HGU) for various rocks near the Swiss Alps, including granite, gneiss, schist, quartzite, hornblende, and ultrabasic rocks. Their results revealed that four granite bodies had HGU values exceeding 10, while all other rock types fell below this level—gneiss measured at 5.8 HGU, and the remaining rocks had values below 4 HGU. Meixner AJ et al. (2014) investigated heat flow in the Cooper Basin of central Australia through gravity inversion and determined that elevated heat flow results from highly heat-producing granites beneath extensive sedimentary layers. Consequently, granite functions as a crucial HDR resource carrier, and its radiogenic heat represents an essential consideration for future HDR surveys.

Granites are widely distributed across South China, and Zhao P et al. (1995) conducted a systematic investigation of their heat generation rates in Southeast China. Their findings revealed an exceptionally high heat production background in the region's granites, with values reaching up to 5.7 $\mu W/m^3$ in certain areas. The region's deep structure shows no evidence of magma chambers serving as additional heat sources. The contemporary geothermal field displays a typical "hot mantle-cold crust" thermal structure, with mantle sources contributing approximately 60% and radioactive decay heat accounting for roughly 40%. However, Lin WJ et al. (2024) demonstrated regional variations in the crustal thermal structure across South China. They observed that in some areas, deep and highly heat-producing granites contribute more to the overall thermal regime than mantle heat flow, resulting in thermal structures characterized as either "hot crust–cold mantle" or "warm crust–warm mantle." Based on the results of drilling HDR exploration wells in South China, future surveys should focus on three key aspects: radioactive heat generation rates of granites of different ages, regional tectonics influencing hydrothermal activities, and the presence of insulating sedimentary cover.

5.2.3. HDR within areas of intense tectonic activity

The Qinghai-Xizang Plateau's uplift, resulting from the India/Asia plate collision, represents one of the most remarkable Cenozoic events. This uplift generated an extensive plateau with surrounding steep mountain chains and doubled the crustal thickness. A distinctive feature of the Qinghai-Xizang Plateau's crustal structure is its low-velocity layer, whose origin remains debated. Current explanations encompass intracrustal partial melting (Hacker BR et al., 2014), crustal ductile shear zones (Paul T et al., 2001), ongoing metamorphism (Shapiro NM et al., 2004), and tectonic superposition (Jiang M et al., 2009). Regardless of its genesis, partial melting or shear heat generation creates a relatively high-temperature characteristic in the low-velocity layer. The correlation between geothermal heat flux density anomalies and the crustal low-velocity layer on the Qinghai-Xizang Plateau (Li ZQ et al., 2005) substantiates the high-temperature nature of this layer, suggesting a potential constant crustal heat source for regional HDR resource formation.

Natural seismic profiles along the Gonghe-Yushu Highway in Qinghai Province indicate a low-velocity layer at 22–41 km depth in the Qiaboqia Valley, where recent HDR resources have been identified in the Gonghe Basin. Zhang C et al. (2018) and Lin WJ et al. (2021) analyzed the heat flow and crustal thermal structure of the Qiaboqia Valley and concluded that this low-velocity layer provides the essential constant heat source for HDR resource formation in the Gonghe Basin. Future HDR exploration on the Qinghai-Xizang Plateau should focus on understanding how the low-velocity layer influences shallow temperature fields and its role as a key source of heat.

5.2.4. HDR within active volcanic areas

China's active volcanoes are predominantly situated in the Tengchong, Leiqiong, Changbaishan, and Wudalianchi regions, with their heat source characteristics intrinsically linked to basal magmatism history and magmatic activity patterns. The Tengchong Volcanic Region represents one of China's most recent volcanic formations, characterized by numerous volcanoes, extensive coverage, diverse eruption types, and sustained volcanic activity from the late Pliocene to the Holocene. Magnetotelluric Sounding (MT) observations indicate three conductive bodies at depths of 10–30 km in the region, potentially representing middle- and lower-crustal magma chambers associated with Tengchong's volcanic activities (Ye T et al., 2018). The Qiongbei region constitutes

one of China's four prominent dormant volcano groups, where stratigraphic imaging reveals a mantle plume beneath Hainan Island extending to the core-mantle boundary (Wei FX et al., 2021). Changbaishan, situated on the Pacific Rim Volcanic Belt, exhibits continuous seismic anomalies in its lower mantle, extending from approximately 660 km depth to the surface, associated with Pacific Plate subduction (Tang YC et al., 2014). The Datong Volcanic Group, developed in the northernmost basin of the Shanxi Graben System, lies within the upper mantle uplift zone of crustal thinning in the North China Craton. Regional imaging and teleseismic waveform data reveal a Y-shaped low-wave velocity anomaly extending from the Datong Volcano Group to the Bohai Sea and into the lower mantle, suggesting a correlation between the Datong volcano formation and Pacific plate subduction (Lei JS, 2012). These regions represent primary targets for active volcanic HDR resource exploration in China. Despite relatively few modern volcanoes, recent discoveries of high-temperature rocks and hydrothermal fluids in the Fushan Depression of the Qiongbei area and the Datong Volcanic Group indicate the presence of unerupted magma (magma capsule) at depth, marking these locations as promising HDR exploration targets.

6. Conclusions

This comprehensive analysis of HDR resource distribution, carbon reduction potential, exploration progress, and EGS construction in China yields the following conclusions:

(i) China possesses abundant HDR resources, with preliminary estimates indicating that heat resources within the 3–10 km depth are equivalent to 8.60×10^{14} t standard coal, thereby further indicating substantial development potential. HDR power generation results in significant carbon reduction advantages compared with traditional coal-fired power generation. Under the baseline scenario, coal-fired power generation generates 0.85 kg CO_2/kWh, while HDR's complete life cycle (including drilling, fracturing, power plant construction, operation, and maintenance) generates only 0.05 kg CO_2/kWh, achieving a 94.4% emission reduction efficiency. Based on the theoretical power generation capacity of 1.67×10^{16} kWh from HDR resources extractable at 3–10 km depth in China, coal power replacement could achieve net emission reductions of 1.34×10^{16} kg CO_2 (approximately 1.34×10^{13} t). Over a 100-year development cycle, this represents average annual emission reductions of 1.34×10^{10} t CO_2, equivalent to 117% of China's 2022 carbon emissions.

(ii) China has achieved significant advances in HDR exploration and development technology, establishing a resource evaluation system and exploration technology framework centered on geophysical exploration, geochemical exploration, and drilling technology. Successfully identified HDR target areas include the Gonghe and North China Basins, where high-temperature HDR has been explored. Breakthroughs in development technology include hydraulic fracturing, microseismic monitoring, and reservoir stimulation. Successful reservoir stimulation in the Gonghe Basin and hydraulic fracturing tests in Matouying have provided valuable experience, paving the way for large-scale HDR development in China.

(iii) As global warming persists, HDR exploitation and utilization, which is feasible in virtually any region worldwide, offers substantial potential for global carbon reduction. However, HDR development faces challenges regarding technical adaptability under complex geological conditions, economic viability, and environmental considerations. Enhanced resource exploration, technological research, and policy support across diverse geological conditions are essential to foster sustainable development of the HDR industry and position it as a key contributor to the global energy transition and environmental sustainability.

CRediT authorship contribution statement

Wen-jing Lin contributed to conceptualization, investigation, data curation, formal analysis, methodology, validation, writing – original draft, software and visualization. Ya-ru Wang contributed to data curation, formal analysis and methodology. Rui Lu contributed to investigation, formal analysis, supervision and funding acquisition. Sheng-sheng Zhang contributed to investigation, data curation, and formal analysis. Gui-ling Wang contributed to conceptualization, formal analysis and funding acquisition.

Declaration of competing interest

The authors declare no conflicts of interest.

Acknowledgments

This study was supported by the National Key Research and Development Program of China (2021YFB1507401), Qinghai Province Clean Energy Minerals Special Project (2022013004qj004) and Geological Survey Project of China Geological Survey (DD20221676, DD20230019). The authors thank LetPub (www.letpub.com.cn) for its linguistic assistance during the preparation of this manuscript.

Supplementary dataset

Supplementary data to this article can been found online at doi: 10.31035/cg2024100.

References

Aghahosseini A, Breyer C. 2020. From hot rock to useful energy: A global estimate of enhanced geothermal systems potential. Applied Energy, 279, 115769. doi: 10.1016/j.apenergy.2020.115769.

Brown DW. 2009. Hot dry rock geothermal energy: Important lessons from Fenton Hill. Stanford University, Stanford, California, 34th Workshop on Geothermal Reservoir Engineering, 139–142.

Cao R, Dor J, Li YB, Meng HR, Cai YQ. 2022. Occurrence characteristics, development status, and prospect of deep high-temperature geothermal resources in China. Chinese Journal of

Engineering, 44(10), 1623–1631 (in Chinese with English abstract). doi: 10.13374/j.issn2095-9389.2022.04.07.003.

Chen KQ, Li ZW, Lin JM, Bao F, Xia X, Xia SH, Lin WJ, Gan HN, Wang LL, Tu GH, Wang H, Bao F. 2022. Crustal magma chamber beneath the Qiongbei volcano field in Hainan Island unveiled by seismic ambient noise tomography. Progress in Geophysics, 37(4), 1379–1391 (in Chinese with English abstract). doi: 10.6038/pg2022DD0501.

Chen MX, Wang JY, Wang JA, Deng X, Yang SZ, Xiong LP, Zhang JM. 1990. The characteristics of the geothermal field and its formation mechanism in the North China down-faulted basin. Acta Geologica Sinica, 64(1), 80–91 (in Chinese with English abstract). doi: 10.19762/j.cnki.dizhixuebao.1990.01.008.

Gao J, Zhang HJ, Zhang SQ, Xin HL, Li ZW, Tian W, Bao F, Cheng ZP, Jia XF, Fu L. 2020. Magma recharging beneath the Weishan volcano of the intraplate Wudalianchi volcanic field, northeast China, implied from 3-D magnetotelluric imaging. Geology, 48(9), 913–918. doi: 10.1130/G47531.1.

Hacker BR, Ritzwoller MH, Xie J. 2014. Partially melted, mica-bearing crust in Central Xizang. Tectonics, 33(7), 1408–1424. doi: 10.1002/2014TC003545.

Hu SB, He LJ, Wang JY. 2000. Heat flow in the continental area of China: A new data set. Earth and Planetary Science Letters, 179(2), 407–419. doi: 10.1016/S0012-821X(00)00126-6.

Jiang GZ, Li WW, Rao S, Shi YZ, Tang XY, Zhu CQ, Gao P, Wang Y, Hu SB. 2016. Heat flow, depth–temperature, and assessment of the enhanced geothermal system (EGS) resource base of continental China. Environmental Earth Sciences, 75(1432), 1–10. doi: 10.1007/s12665-016-6238-5.

Jiang HY, Wang SX, Kang FX, Shi M, Fan ZH, Zhang L. 2019. Geological characteristics and resource potential of dry-hot pore ZKCW01 in Wendeng, Shandong Province. Acta Geologica Sinica, 93(s1), 217–225 (in Chinese with English abstract). doi: 10.19762/i.cnki.dizhixuebao.2019231.

Jiang M, Wang YX, Qian H. 2009. Plateaus of mountain building - Broadband seismic sounding and upper crustal mantle structure of the Xizang Plateau and its adjacent areas. Beijing, Geological Press, 1–209 (in Chinese).

Koelbel T, Genter A. 2017. Enhanced geothermal systems: The Soultz-sous-Forêts project. Cham, Springer, 243–248. doi: 10.1007/978-3-319-45659-1_25.

Kong YL, Pan S, Ren YQ, Zhang WZ, Wang K, Jiang GZ, Cheng YZ, Sun WJ, Zhang C, Hu SB. 2021. Catalog of enhanced geothermal systems based on heat sources. Acta Geologica Sinica-English Edition, 95(6), 1882–1891. doi: 10.1111/1755-6724.14876.

Laske G, Masters G, Ma Z, Pasyanos M. 2013. Update on CRUST1. 0-A 1-degree global model of Earth's crust. Geophysical Research Abstracts, 15, Abstract EGU2013-Abstract EGU2658.

Lei JS. 2012. Upper‐mantle tomography and dynamics beneath the North China Craton. Journal of Geophysical Research: Solid Earth, 95(6), 1882–1891. doi: 10.1029/2012JB009212.

Li DW, Wang YX. 2015. Major issues of research and development of hot dry rock geothermal energy. Earth Science, 40(11), 1858–1869 (in Chinese with English abstract). doi: 10.3799/dqkx.2015.166.

Li WB. 2016. Hot dry rock resource potential assessment in Cangxian Anticlise Zone, Hebei Province. Coal Geology of China, 28(11), 43–48 (in Chinese with English abstract). doi: 10.3969/j.issn.1674-1803.2016.11.09.

Li X, Qi XF, Shangguan ST, Su Y, Tian XF, Tian LL, Pan MM, Song GL. 2022. Application of ORC power generation system in hot dry rock pilot power generation. Coal Geology of China, 34(7), 12–15 (in Chinese with English abstract). doi: 10.3969/j.issn.1674-1803.2022.07.03.

Li ZQ, Hou ZQ, Nie FJ, Meng XJ. 2005. Characteristic and distribution of the partial melting layers in the upper crust: Evidence from active hydrothermal fluid in the south Xizang. Acta Geologica Sinica, 79(1), 68–77 (in Chinese with English abstract). doi: 10.3321/j.issn:0001-5717.2005.01.008.

Liao ZJ. 2012. Deep-circulation hydrothermal systems without magmatic heat source in Fujian Province. Geoscience, 26(1), 85–98 (in Chinese with English abstract). doi: 10.3969/j.issn.1000-8527.2012.01.009.

Lin WJ, Liu ZM, Ma F, Liu CL, Wang GL. 2012. Potential estimation of HDR resources of mainland China. Acta Geoscientica Sinica, 33(5), 807–811 (in Chinese with English abstract). doi: 10.3975/cagsb.2012.05.12.

Lin WJ, Wang GL, Gan HN. 2024. Differential crustal thermal structure and geothermal significance in the igneous region of southeastern China. Acta Geologica Sinica, 98(2), 544–557 (in Chinese with English abstract). doi: 10.19762/j.cnki.dizhixuebao.2023027.

Lin WJ, Wang GL, Gan HN, Wang AD, Yue GF, Long XT. 2022. Heat generation and accumulation for Hot Dry Rock resources in the igneous rock distribution areas of southeastern China. Lithosphere, 2021(Special 5), 2039112. doi: 10.2113/2022/2039112.

Lin WJ, Wang GL, Gan HN, Zhang SS, Zhao Z, Yue GF, Long XT. 2023. Heat source model for Enhanced Geothermal Systems (EGS) under different geological conditions in China. Gondwana Research, 122, 243–259. doi: 10.1016/j.gr.2022.08.007.

Lin WJ, Wang GL, Zhang SS, Zhao Z, Xing LX, Gan HN, Tan XF. 2021. Heat aggregation mechanisms of hot dry rocks resources in the Gonghe Basin, Northeastern Xizang Plateau. Acta Geologica Sinica‐English Edition, 95(6), 1793–1804. doi: 10.1111/1755-6724.14873.

Liu CL, Lu CM, Li YS, Hao QC, Cao SW. 2022. Genetic model and exploration target area of geothermal resources in Hongtang Area, Xiamen, China. Journal of Groundwater Science and Engineering, 10(2), 128–137. doi: 10.19637/j.cnki.2305-7068.2022.02.003.

Liu LX, Lu R, Xie WP, Liu B, Wang YR, Yao HH, Lin WJ. 2024. Distribution and hydrogeochemical characteristics of hot springs in northeastern Xizang Plateau. Earth Science Frontiers, 31(6), 173–195 (in Chinese with English abstract). doi: 10.13745/j.esf.sf.2024.7.17.

Long XT, Wang GL, Lin WJ, Wang J, He ZQ, Ma JC, Yin XF. 2023. Locating geothermal resources using seismic exploration in Xian County, China. Geothermics, 112, 102747. doi: 10.1016/j.geothermics.2023.102747.

Lu R, Xie WP, Liu B, Zhang SS, Zhu JS, Lin WJ. 2024. Geothermal fluid chemistry and isotope for interpreting the formation of complex geothermal system in the Gonghe Basin, northeastern Xizang Plateau. Journal of Hydrology, 633, 130813. doi: 10.1016/j.jhydrol.2024.130813.

Mao XM, Wang YX, Yuan JF. 2013. The indication of geothermal events by helium and carbon isotopes of hydrothermal fluids in South China. Procedia Earth and Planetary Science, 7, 550–553. doi: 10.1016/j.proeps.2013.03.163.

Mao XP, Li KW, Wang XW. 2019. Causes of geothermal fields and characteristics of ground temperature fields in China. Journal of Groundwater Science and Engineering, 7(1), 15–28. doi: 10.19637/j.cnki.2305-7068.2019.01.002.

Mao XP, Wang XW, Li KW, Guo SB. 2018. Sources of heat and control factors in geothermal field. Earth Science, 43(11), 4256–4266 (in Chinese with English abstract). doi: 10.3799/dqkx.2018.210.

Meixner AJ, Kirkby AL, Horspool N. 2014. Using constrained gravity inversions to identify high-heat-producing granites beneath thick sedimentary cover in the Cooper Basin region of central Australia. Geothermics, 51, 483–495. doi: 10.1016/j.geothermics.2013.10.010.

Moore J, McLennan J, Allis R, Pankow K, Simmons S, Podgorney R, Wannamaker P, Bartley J, Jones C, Rickard W. 2019. The Utah Frontier Observatory for Research in Geothermal Energy (FORGE): An international laboratory for enhanced geothermal system

technology development. Stanford University, Stanford, California, 44th workshop on geothermal reservoir engineering, 11–13.

Paul T, Xu ZQ, Françoise R, Bertrand M, Nicolas A, Gérard W, Yang J. 2001. Oblique Stepwise Rise and Growth of the Xizang Plateau. Science, 294(5547), 1671–1677. doi: 10.1126/science.105978.

Qi XF, Shangguan ST, Zhang GB, Pan MM, Su Y, Tian LL, Xiang L, Qiao YC, Zhang JY. 2020. Site selection and developmental prospect of hot dry rock resources project in the Matouying uplift, Hebei Province. Earth Science Frontiers, 27(1), 94–102 (in Chinese with English abstract). doi: 10.13745/j.esf.2020.1.11.

Qin XX, Zhang M, Ye J, Liu HM, Wang GL, Shi JS. 2019. ORC Power generation and integrated cascade utilization of medium-low temperature geothermal resources in Cangxian Bulge region, Hebei Province. Acta Geoscientica Sinica, 40(2), 307–313 (in Chinese with English abstract). doi: 10.3975/cagsb.2019.011101.

Qiu NS. 1998. Thermal status profile in the terrestrial sedimentary basin in China. Advances in Earth Science, 13(5), 447–451 (in Chinese with English abstract). doi: 10.11867/j.issn.1001-8166.1998.05.0447.

Rybach L, Bodmer P, Pavoni N, Mueller S. 1978. Siting criteria for heat extraction from hot dry rock: Application to Switzerland. Pure and Applied Geophysics, 116(6), 1211–1224. doi: 10.1007/BF00874681.

Shapiro NM, Ritzwoller MH, Molnar P, Levin V. 2004. Thinning and flow of Xizang crust constrained by seismic anisotropy. Science, 305(5681), 233–236. doi: 10.1126/science.1098276.

Sigurjónsson HÆ, Cook D, Davíðsdóttir B, Bogason SG. 2021. A life-cycle analysis of deep enhanced geothermal systems – The case studies of Reykjanes, Iceland and Vendenheim, France. Renewable Energy, 177, 1076–1086. doi: 10.1016/j.renene.2021.06.013.

Sun ZX, Li BX, Wang ZL. 2011. Exploration of the possibility of hot dry rock occurring in the Qinghai Gonghe Basin. Hydrogeology & Engineering Geology, 38(2), 119–124 (in Chinese with English abstract). doi: 10.16030/j.cnki.issn.1000-3665.2011.02.030.

Tan XF, Liu X, Wang GL, Wang H. 2020. Research on the key technology for the investigation and evaluation of the hot dry rock geothermal resources in Lijin. Acta Geologica Sinica, 94(7), 2166–2176 (in Chinese with English abstract). doi: 10.19762/j.cnki.dizhixuebao.2020233.

Tang YC, Obayashi M, Niu FL, Grand SP, Chen YJ, Kawakatsu H, Tanaka S, Ning JY, Ni JF. 2014. Changbaishan volcanism in northeast China linked to subduction-induced mantle upwelling. Nature Geoscience, 7(6), 470–475. doi: 10.1038/ngeo2166.

Teng JW, Si X, Zhuang QX, Liu YS, Yan YF, Zhao BB, Zheng SG, Liu SH. 2017. Abnormal structure of crust and mantle and analysis of deep thermal potential in Fujian continental margin. Science Technology and Engineering, 17(17), 6–38 (in Chinese with English abstract).

Tester JW, Anderson BJ, Batchelor AS, Blackwell DD, DiPippo R, Drake EM, Garnish J, Livesay B, Moore MC, Nichols K. 2006. The future of geothermal energy. Massachusetts Institute of Technology, 358, 1–3. doi: 10.2172/1220063.

Tian J, Li YM, Zhou XC, Pang ZH, Li LW, Xing LT, Li ZP. 2021. Geochemical characteristics of hydrothermal volatiles from Southeast China and their implications on the tectonic structure controlling heat convection. Frontiers in Earth Science, 9. doi: 10.3389/feart.2021.786051.

Wan TF, Chu MJ, Chen MY. 1988. Thermal regimes of the lithophere and geothermal resources potential in Fujian Province. Acta Geologica Sinica, (2), 178–189 (in Chinese with English abstract). doi: 10.19762/j.cnki.dizhixuebao.1988.02.008.

Wan ZJ, Zhao YS, Kang JR. 2005. Forecast and evaluation of hot dry rock geothermal resource in China. Renewable Energy, 30(12), 1831–1846. doi: 10.1016/j.renene.2005.01.016.

Wang GL, Gan HN, Lin WJ, Yue GF, Yan XX, Li TX, Zhang W, Ma F. 2023a. Hydrothermal Systems Characterized by Crustal Thermally-dominated Structures of Southeastern China. Acta Geologica Sinica - English Edition, 97(4), 1003–1013. doi: 10.1111/1755-6724.15078.

Wang GL, Lin WJ. 2020. Main hydro-geothermal systems and their genetic models in China. Acta Geologica Sinica, 94(7), 1923–1937 (in Chinese with English abstract). doi: 10.19762/j.cnki.dizhixuebao.2020224.

Wang GL, Lin WJ, Liu F, Wang SQ, Yue GF, Long XT, Liu YG. 2023b. Theory and survey practice of deep heat accumulation in geothermal system and exploration practice. Acta Geologica Sinica, 97(3), 639–660 (in Chinese with English abstract). doi: 10.19762/j.cnki.dizhixuebao.2023016.

Wang GL, Lin WJ, Zhang W, Lu C, Ma F, Gan HN. 2016. Research on Formation Mechanisms of Hot Dry Rock Resources in China. Acta Geologica Sinica - English Edition, 90(4), 1418–1433. doi: 10.1111/1755-6724.12776.

Wang GL, Liu YG, Duan HX, Liu ZY, Hu J, Bian K, Xing LX. 2023c. Crust-mantle differentiation and thermal accumulation mechanisms in the north China plain. Renewable Energy, 213, 63–74. doi: 10.1016/j.renene.2023.05.136.

Wang L, Jia LQ. 2024. Carbon emission reduction: Contribution of geothermal energy and practice in China. China Geology, 7(1), 161–164. doi: 10.31035/cg2023088.

Wang N, Ren YX, Zhu T, Meng FX, Wen ZG, Liu GY. 2018. Life cycle carbon emission modelling of coal-fired power: Chinese case. Energy, 162, 841–852. doi: 10.1016/j.energy.2018.08.054.

Wang S, Kuang J, Huang XL, Zhang HY, Zhang M, Qi SH, Han YJ, Xiao ZC, Wang SQ, Tang L. 2022. Upwelling of Mantle-derived Material in Southeast China: Evidence from Noble Gas Isotopes. Acta Geologica Sinica - English Edition, 96(1), 100–110. doi: 10.1111/1755-6724.14686.

Wang XW, Gao NA, Wang TH, Liu HY, Mao XP, Huang X. 2022. Distribution characteristics and genetic mechanism of the geothermal abnormality in the Xianxian geothermal field, Hebei Province. Acta Geologica Sinica, 96(7), 2611–2625 (in Chinese with English abstract). doi: 10.19762/j.cnki.dizhixuebao.2021278.

Wei FX, Wei W, Yu HM. 2021. The Cenozoic volcanic fields in northern Hainan Island and the Leizhou Peninsula, south China: Eruption history, magma source and dynamic background. Geological Society of London, 179–198. doi: 10.1144/SP510-2020-64.

Xu TF, Xu L, Yi X, Jiang ZJ, Fabrizio G. 2022. Performance evaluation of the Habanero enhanced geothermal system, Australia: Optimization based on tracer and induced micro-seismicity data. Renewable Energy, 181, 1197–1208. doi: 10.1016/j.renene.2021.09.111.

Yan WD. 2015. Characteristics of Gonghe Basin hot dry rock and its utilization prospects. Science & Technology Review, 33(19), 54–57 (in Chinese with English abstract). doi: 10.3981/j.issn.1000-7857.2015.19.008.

Yao YH, Jia XF, Li ST, Cui JY, Xiang H, Yue DD, Zhang QX, Feng ZL. 2025. Quantitative study on vertical distribution of heat flow in Niutuozhen geothermal field, Xiong'an New Area—Evidence from heat flow determination in the Archean of D01 well. Journal of Groundwater Science and Engineering, 13(1), 22–33. doi: 10.26599/JGSE.2025.9280036.

Ye T, Huang QH, Chen XB, Zhang HQ, Chen YJ, Zhao L, Zhang Y. 2018. Magma Chamber and Crustal Channel Flow Structures in the Tengchong Volcano Area From 3-D MT Inversion at the Intracontinental Block Boundary Southeast of the Xizang Plateau. Journal of Geophysical Research: Solid Earth, 123(12), 11–111–112,126. doi: 10.1029/2018JB015936.

Yin XX, Shen J, Zhao YT, Liu DL, Zhao SM, Zong ZH. 2021. Study on tracer test of carbonate geothermal reservoir under centralized pumping and re-injection conditions. Acta Geologica Sinica, 95(6), 1984–1994 (in Chinese with English abstract). doi: 10.19762/j.

cnki.dizhixuebao.2021041.

Yin XX, Zhao SM, Cai Y, Yan JX, Xu L. 2024. Characterization of thermal storage dynamics of large-scale geothermal development in Tianjin in the last thirty years. Acta Geologica Sinica, 98(1), 297–313 (in Chinese with English abstract). doi: 10.19762/j.cnki.dizhixuebao.2023017.

Zarrouk SJ, Moon H. 2014. Efficiency of geothermal power plants: A worldwide review. Geothermics, 51, 142–153. doi: 10.1016/j.geothermics.2013.11.001.

Zhang C, Jiang GZ, Shi YZ, Wang ZT, Wang Y, Li ST, Jia XF, Hu SB. 2018. Terrestrial heat flow and crustal thermal structure of the Gonghe-Guide area, northeastern Qinghai-Xizang plateau. Geothermics, 72, 182–192. doi: 10.1016/j.geothermics.2017.11.011.

Zhang EY, Wen DG, Wang GL, Yan WD, Wang WS, Ye CM, Li XF, Wang H, Tang XC, Weng W, Li K, Zhang CY, Liang MX, Luo HB, Hu HY, Zhang W, Zhang SQ, Jin XP, Wu HD, Zhang LY, Feng QD, Xie JY, Wang D, He YC, Wang YW, Chen ZB, Cheng ZP, Luo WF, Yang Y, Zhang H, Zha EL, Gong YL, Zheng Y, Jiang CS, Zhang SS, Niu X, Zhang H, Hu LS, Zhu GL, Xu WH, Niu ZX, Yang L. 2022. The first power generation test of hot dry rock resources exploration and production demonstration project in the Gonghe Basin, Qinghai Province, China. China Geology, 5(3), 372–382. doi: 10.31035/cg2022038.

Zhang FS, Cao ST, An MK, Zhang CY, Elsworth D. 2023. Friction and stability of granite faults in the Gonghe geothermal reservoir and implications for injection-induced seismicity. Geothermics, 112, 102730. doi: 10.1016/j.geothermics.2023.102730.

Zhang SS, Zhang L, Tian CC, Cai JC, Tang BC. 2019. Occurrence geological characteristics and development potential of hot dry rocks in Qinghai Gonghe basin. Journal of Geomechanics, 25(4), 501–508 (in Chinese with English abstract). doi: 10.12090/j.issn.1006-6616.2019.25.04.048.

Zhang W, Wang G, Liu F, Xing L, Li M. 2019. Characteristics of geothermal resources in sedimentary basins. Geology in China, 46(2), 255–268 (in Chinese with English abstract). doi: 10.12029/gc20190204.

Zhang XB, Hu QH. 2018. Development of geothermal resources in China: A review. Journal of Earth Science, 29(2), 452–467. doi: 10.1007/s12583-018-0838-9.

Zhao P, Wang JY, Wang JA, Luo DG. 1995. Characteristics of heat production distribution in SE China. Acta Petrologica Sinica (3), 292−305 (in Chinese with English abstract).

Zhao YD, Gan HJ, Shi Y, Chen SB, Wang GH. 2016. Characteristics of geothermal anomaly and its effect on oil and gas reservoir in Fushan sag of Beibuwan Basin. Petroleum Geology and Recovery Efficiency, 23(3), 40–46 (in Chinese with English abstract). doi: 10.13673/j.cnki.cn37-1359/te.20151215.001.

Zhou WL, Hu XY, Guo HD, Liu S, Liu SJ, Yang B. 2022. Three-dimensional magnetotelluric inversion reveals the typical geothermal structure of Yanggao geothermal field in Datong Basin, northern China. Geothermics, 105, 102505. doi: 10.1016/j.geothermics.2022.102505.

Zhou ZM, Ma CQ, Qi SH, Xi YF, Liu W. 2020. Late Mesozoic high-heat-producing (HHP) and high-temperature geothermal reservoir granitoids: The most significant geothermal mechanism in South China. Lithos, 366−367, 105568. doi: 10.1016/j.lithos.2020.105568.